https://doi.org/10.5194/bg-2019-500
Preprint. Discussion started: 11 March 2020

Biogeosciences Discussions
Open Access
EGU

Assessing branched tetraether lipids as tracers of soil organic carbon transport through the Carminowe Creek catchment (southwest England)

Jingjing Guo[1], Miriam Glendell[2], Jeroen Meersmans[3], Frédérique Kirkels[1], Jack J Middelburg[1], Francien Peterse[1]

[1]Department of Earth Sciences, Utrecht University, 3584 CB Utrecht, the Netherlands
[2]The James Hutton Institute, Aberdeen, AB15 8QH, UK
[3]TERRA Teaching and Research Centre, Gembloux Agro-Bio Tech, University of Liege, 5030 Gembloux, Belgium

Correspondence to: Jingjing Guo (j.guo@uu.nl)

In preparation for submission to: Biogeosciences

Abstract. Soils represent the largest reservoir of organic carbon (OC) on land. Upon mobilization, this OC is either returned to the atmosphere as carbon dioxide (CO_2), or transported and ultimately locked into (marine) sediments, where it will act as a long-term sink of atmospheric CO_2. These fluxes of soil OC are, however, poorly quantified, mostly due to the lack of a soil-specific tracer. In this study, a suite of branched glycerol dialkyl glycerol tetraethers (brGDGTs), which are membrane lipids of soil bacteria, is tested as specific tracers for soil OC from source (soils under arable land, ley, grassland and woodland) to sink (Lake Loe Pool sediments) considering a small catchment located in southwest England (i.e. Carminowe Creek draining into Lake Loe Pool). The analysis of brGDGTs in catchment soils reveals that their distribution is not significantly different across different land use types ($p > 0.05$), and thus does not allow tracing land use-specific soil contributions to Lake Loe Pool sediments. Furthermore, the significantly higher contribution of 6-methyl brGDGT isomers in creek sediments (isomerization ratio (IR) = 0.48 ± 0.10; mean ± s.d., standard deviation; $p < 0.05$) compared to that in catchment soils (IR = 0.28 ± 0.11) indicates that the initial soil signal is substantially altered by brGDGT produced *in situ*. Similarly, the riverine brGDGT signal appears to be overwritten by lacustrine brGDGTs in the lake sedimentary record, indicated by remarkably lower Methylation of Branched Tetraethers (MBT'_{5ME} = 0.46 ± 0.02 in creek bed sediment and 0.38 ± 0.01 in lake core sediment; $p < 0.05$) and higher Degree of Cyclization (DC = 0.23 ± 0.02 in creek bed sediment and 0.32 ± 0.08 in lake core sediment). Thus, in this small catchment, brGDGTs do not allow us to trace soil OC transport. Nevertheless, the downcore changes in the degree of cyclization and the abundance of isoprenoid GDGTs produced by methanogens in the Lake Loe Pool sediment do reflect local environmental conditions over the past 100 years, and have recorded the eutrophication history of the lake.

https://doi.org/10.5194/bg-2019-500
Preprint. Discussion started: 11 March 2020

Biogeosciences Discussions

1 Introduction

Globally, around 1500–2000 Pg of carbon is stored in soils in the form of organic matter, which is about two times the amount of carbon in the atmosphere and three times the amount of carbon in vegetation (Janzen, 2004; Smith, 2008). Soil organic carbon (OC) plays an important role in the global carbon cycle, as subtle alterations in the soil OC reservoir may affect the concentration of atmospheric CO_2 and thus influence climate change (Davidson and Janssens, 2006). Atmospheric CO_2 that is fixed by plants through photosynthesis will be stored into soil OC pool, part of which will be transferred to streams and rivers. Upon fluvial discharge, soil OC is buried and locked into the marine or lacustrine sediment, where it will act as a long-term carbon sink. However, instead of a passive pipeline in the carbon cycle, rivers actually represent a dynamic channel, where part of the soil OC is respired back to the atmosphere, and another part may be stored in river bed or lake sediments before reaching the ocean (Cole et al., 2007; Battin et al., 2009; Aufdenkampe et al., 2011). Hence, it is hard to determine the exact amount of soil OC that is transported to the ocean, as the dynamic processes that soil OC undergoes during transport, such as degradation and sequestration, are elusive. This is mostly due to the lack of a specific tracer to distinguish soil OC from the total pool of OC that is also comprised of plant-derived OC, aquatic produced OC, and fossil OC from rock erosion (Blair et al., 2004; Aufdenkampe et al., 2011).

To circumvent this problem, lipid biomarkers can be used to trace a specific part of the total OC pool in complex natural environmental systems (Brassell and Eglinton, 1986; Wakeham and Lee, 1993). For example, odd-numbered long chain *n*-alkanes derived from epicuticular plant waxes are widely used to detect the contribution of terrestrial OC to river-dominated marine sediments (Eglinton and Hamilton, 1967; Hedges et al., 1997; Fernandes and Sicre, 2000; Glendell et al., 2018). Similarly, lignin, an abundant biopolymer in vascular plants (Hedges et al., 1997), has been used to trace OC transport along the terrestrial-aquatic continuum by e.g., in the Mississippi River (Goñi et al., 1997; Bianchi et al., 2004), the Amazon Rivers (Hedges et al., 1986, 2000; Feng et al., 2016), and Arctic rivers (Feng et al., 2013). However, these biomarkers are derived from vegetation, which, although land-derived, is not fully representative of soil OC. Thus, in order to specifically trace and quantify the pool of soil OC, another biomarker is needed.

Branched glycerol dialkyl glycerol tetraethers (brGDGTs; Fig. 1) are membrane spanning tetraether lipids synthesized by heterotrophic bacteria that thrive in soils and peats all over the world (Weijers et al., 2006a, 2007a; Naafs et al., 2017a). Although the exact producers of these lipids are still unknown, after the detection of a brGDGT in an Acidobacterial culture (Sinninghe Damsté et al., 2011, 2014, 2018), it was assumed that Acidobacteria are the source organisms of brGDGTs. The occurrence and relative distribution of brGDGTs in a global set of modern surface soils showed that they can have 4 to 6 methyl groups attached to their alkyl backbone, where the degree of branching increases in soils from colder areas. Furthermore, brGDGTs respond to changes in soil pH by forming up to 2 cyclopentane moieties following internal cyclization, where a higher number of cyclopentane moieties corresponds to a higher soil pH (Weijers et al., 2007a). Initially, a combination of two indices, the Methylation of Branched Tetraethers (MBT) index and Cyclization of Branched

https://doi.org/10.5194/bg-2019-500
Preprint. Discussion started: 11 March 2020

Tetraethers (CBT) index, was proposed as a proxy to reconstruct the mean air temperature (MAT) and pH of a soil (Weijers et al., 2007a; Peterse et al., 2012). After the identification of novel brGDGT isomers that possess a methyl group at the α and/or ω 6 position rather than at position 5 (Fig. 1) and the improvement of the chromatography method used for brGDGT analysis, a modified temperature proxy, the MBT'_{5ME} was developed (De Jonge et al., 2013, 2014b). Furthermore, the relative abundance of 6-methyl brGDGT isomers, quantified as the Isomerization Ratio (IR), appeared to also relate to soil pH (De Jonge et al., 2014a). Indeed, the analysis of brGDGTs in peat profiles and loess-paleosol sequences has resulted in long-term continental paleotemperature records for various areas, e.g. in deglacial central China (Peterse et al., 2011) and northeast China (Zheng et al., 2017), and western Europe during the early Eocene (Inglis et al., 2017).

These brGDGTs have not only been found in soils, but also in coastal marine sediments, where they have been used as the terrestrial end-member in the Branched and Isoprenoid Tetraether (BIT) index that determines the relative contribution of fluvially supplied soil organic matter to marine sediments, where the latter is represented by amounts of the isoprenoid GDGT crenarchaeol (Hopmans et al., 2004). For example, the relative abundance of brGDGTs in a marine sediment core from the Bay of Biscay revealed the early re-activation of European rivers after the last deglaciation (Ménot et al., 2006). Furthermore, brGDGTs stored in continental margin sediments are assumed to represent an integrated climate signal of the nearby land, and have been used as such to generate temperature records of deglacial tropical Africa (Weijers et al., 2007b), and Pliocene North-Western Europe (Dearing Crampton-Flood et al., 2018).

Recently, however, brGDGTs have also been found to be produced in aquatic systems such as coastal marine areas (Peterse et al., 2009b; Sinninghe Damsté, 2016), rivers (Zell et al., 2013, 2014a) and lakes (Sinninghe Damsté et al., 2009a; Tierney and Russell, 2009; Loomis et al., 2011, 2014; Schoon et al., 2013; Weber et al., 2015, 2018), which complicates the interpretation of brGDGT-based proxies. Aquatic production became apparent upon comparison of brGDGTs in Svalbard fjord sediments and nearby soils. Whereas the brGDGT signal in the fjord sediments was dominated by compounds containing cyclopentane moieties, soils where characterized by brGDGTs without cyclization (Peterse et al., 2009b). These substantially different brGDGT signatures in combination with the increasing concentration of brGDGTs towards the open ocean then pointed towards a contribution of *in situ* produced brGDGTs to the fjord sediments. Similarly, De Jonge et al. (2014a) found that brGDGTs in suspended particulate matter (SPM) from the Yenisei River matched better with the pH of the river water than that of the soils in the river catchment. Also, the distribution of brGDGTs in SPM remained constant, whereas the Yenisei catchment spans a large latitudinal range with a large range in temperature, which led them to conclude that the majority of the brGDGTs in SPM are produced in the river. Notably, these and subsequent studies proposed ways to recognize *in situ* production of brGDGTs in aquatic environments. For example, the aquatic brGDGTs in the Yenisei River were characterized by a relatively high contribution of 6-methyl brGDGT isomers (De Jonge et al., 2014a), whereas a high degree of cyclization is an indicator of brGDGT production in coastal marine zones (Peterse et al., 2009b; Sinninghe

https://doi.org/10.5194/bg-2019-500
Preprint. Discussion started: 11 March 2020

Damsté, 2016), for which Sinninghe Damsté (2016) proposed that a weighed number of rings in tetramethylated brGDGTs, quantified as $\#rings_{tetra} > 0.7$ indicates a purely marine source of brGDGTs in continental margin sediments.

Here we test brGDGTs as tracers for soil OC in Carminowe Creek catchment, a small catchment in southwest England. Previously, an attempt was made to follow OC transport from soil (source) to Lake Loe Pool, the final sink of this catchment, using a combination of stable isotopes of bulk soil OC and plant leaf wax *n*-alkanes as fingerprints for the different vegetation types present in the catchment (i.e. arable land, grassland, ley and woodland) (Glendell et al., 2018). Although most land use types had a distinct *n*-alkane fingerprint, OC derived from arable land and temporary grassland (ley) could not be distinguished (Glendell et al., 2018). Hence, the analysis of brGDGTs in the same samples may contribute to tracing soil OC from different land use types during transport in Carminowe Creek. Moreover, changes in brGDGT distributions in a 50 cm long sediment core from Loe Pool can be used to infer changes in soil OC transport dynamics in the catchment over the past century, and potentially couple them to climate or anthropogenic activity related events in the catchment area.

2 Methods

2.1 Study site and sampling

An overview of the study area and sampling sites is given by Glendell et al. (2018). Briefly, the Carminowe Creek catchment is located in Cornwall in southwest England (50°14' N, 5°16' W), covers an area of around 4.8 km^2 and varies in elevation from 0 to 80 m above sea level (Fig. 2). It is divided into two subcatchments ('north' and 'south'). The two streams converge around 100 m before their joint outlet, and then flow into a natural freshwater lake Loe Pool (50 ha), which is separated from the Atlantic Ocean by a natural shingle barrier. The mean annual temperature (MAT) and mean annual precipitation (MAP) in this area are approximately 11 °C and 1000 mm $year^{-1}$, respectively. The land use in this studied catchment is dominated by arable land and temporary grasslands (ley), which are under rotation. The steeper hillslopes are under permanent grassland, and riparian woodland covers the areas near the creek. For this study, 74 surface soil samples (0–15 cm) were collected along 14 hillslope transects, including 31 arable land sites, 14 permanent grassland sites, 24 temporary grassland (ley) sites and 5 woodland sites (Fig. 2). Riverbed sediments were collected at three locations along each of the two tributaries (upstream, midstream and downstream), and one more at the joint outlet. A 50 cm long sediment core was taken in the lake, about 150 m away from the joint outlet. The lake core has been dated by the activity of Caesium-137 (^{137}Cs), and it covers the last 100 years (Glendell et al., 2018).

2.2 Bulk soil properties

Total carbon contents were reported by Glendell et al. (2018). Soil pH was measured in this study using a pH meter in a soil to water ratio of 1:5 (w:v) after shaking for two hours.

https://doi.org/10.5194/bg-2019-500
Preprint. Discussion started: 11 March 2020


Biogeosciences Discussions Open Access EGU

2.3 GDGT extraction and analysis

In total, 74 soil samples, 7 creek bed sediment and 25 lake core sediment samples were analysed for GDGTs. First, 5–7 g of the soils or 3–5 g of the sediments were freeze dried and homogenized, after which they were extracted three times with dichloromethane (DCM) : MeOH (9 : 1, v/v) using an accelerated solvent extractor (ASE 350, Dionex^{TM}) at 100 °C and 7.7 × 10^6 Pa to obtain a total lipid extract (TLE). After addition of a known amount of C_{46} GDGT internal standard (Huguet et al., 2006), the TLEs were dried under a N_2 stream, and then separated into apolar and polar fractions by passing them over an activated Al_2O_3 column using hexane : DCM (9 : 1, v/v) and DCM : MeOH (1 : 1, v/v) respectively. The polar fraction, which contains the GDGTs, was evaporated to dryness under a gentle N_2 stream. After this, the samples were prepared for further analysis by re-dissolving them in a hexane : isopropanol (99 : 1, v/v) mixture, and filtration through a 0.45 μm polytetrafluoroethylene (PTFE) filter.

The GDGTs were analysed on an Agilent 1260 Infinity ultra high performance liquid chromatography (UHPLC) coupled to an Agilent 6130 single quadrupole mass spectrometer (MS) with settings according to Hopmans et al. (2016). The GDGTs were separated over two silica Waters Acquity UPLC BEH Hilic columns (1.7 μm, 2.1 mm x 150 mm) preceded by a guard column with the same packing. GDGTs were eluted isocratically at a flow rate of 0.2 ml min^{-1} using 82% A and 18% B for 25 min, followed by a linear gradient to 70% A and 30% B for 25 min, where A = hexane and B = hexane : isopropanol (9 : 1, v/v). Sample injection volumes were 10 μL. Ionization of the GDGTs was achieved by atmospheric pressure chemical ionization with the following source settings: gas temperature 200 °C, vaporizer temperature 400 °C, N_2 flow 6 L min^{-1}, capillary voltage 3500 V, nebulizer pressure 25 psi and a corona current of 5.0 μA. By scanning the $[M+H]^+$ ions (protonated mass) in selected ion monitoring (SIM) mode, the target compounds were detected at *m/z* 1302 (GDGT-0), 1292 (crenarchaeol), 1050 (brGDGT–IIIa), 1048 (brGDGT–IIIb), 1046 (brGDGT–IIIc), 1036 (brGDGT–IIa), 1034 (brGDGT–IIb), 1032 (brGDGT–IIc), 1022 (brGDGT–Ia), 1020 (brGDGT–Ib), 1018 (brGDGT–Ic), with *m/z* 744 for the internal standard. Quantitation was achieved by peak area integration of the $[M+H]^+$ ions in Chemstation software B.04.03.

2.4 GDGT proxy calculations

The roman numerals in following equations refer to the molecular structures of GDGTs in Fig.1. The ratios below were calculated based on the fractional abundances (indicated by using square brackets) of GDGTs. The BIT index was calculated according to Hopmans et al. (2004), and modified to also include 6-methyl brGDGTs:

$$BIT = \frac{[Ia]+[IIa]+[IIIa]+[IIa']+[IIIa']}{[Ia]+[IIa]+[IIIa]+[IIa']+[IIIa']+[crenarchaeol]} \quad (1)$$

The degree of methylation (MBT'_{5ME}) and relative abundances of tetra-, penta-, and hexamethylated brGDGTs were calculated following De Jonge et al. (2014b) and Sinninghe Damsté et al. (2016):

https://doi.org/10.5194/bg-2019-500
Preprint. Discussion started: 11 March 2020

$$MBT'_{5Me} = \frac{[Ia]+[Ib]+[Ic]}{[Ia]+[Ib]+[Ic]+[IIa]+[IIb]+[IIc]+[IIIa]} \quad (2)$$

$$\%tetra = \sum[tetramethylated\ brGDGTs] = [Ia] + [Ib] + [Ic] \quad (3)$$

$$\%penta = \sum[pentamethylated\ brGDGTs] = [IIa] + [IIb] + [IIc] + [IIa'] + [IIb'] + [IIc'] \quad (4)$$

$$\%hexa = \sum[hexamethylated\ brGDGTs] = [IIIa] + [IIIb] + [IIIc] + [IIIa'] + [IIIb'] + [IIIc'] \quad (5)$$

Furthermore, the degree of cyclization (DC) was calculated according to Baxter et al. (2019):

$$DC = \frac{[Ib]+2*[Ic]+[IIb]+[IIb']}{[Ia]+[Ib]+[Ic]+[IIa]+[IIa']+[IIb]+[IIb']} \quad (6)$$

The isomerization ratio (IR) is the ratio between penta- and hexamethylated 6-methyl brGDGTs and the total amount of both 5- and 6-methyl penta- and hexamethylated brGDGTs (De Jonge et al., 2014a):

$$IR = \frac{[IIa']+[IIb']+[IIc']+[IIIa']+[IIIb']+[IIIc']}{[IIa]+[IIa']+[IIb]+[IIb']+[IIc]+[IIc']+[IIIa]+[IIIa']+[IIIb]+[IIIb']+[IIIc]+[IIIc']} \quad (7)$$

2.5 Statistical analysis and data visualization

The statistical analysis and data visualization were undertaken in R programming (version 3.5.2) (R Core Team, 2018). Differences in the concentration of brGDGTs and brGDGT-based indices between different land use types (i.e. arable land, grassland, ley and woodland), creek bed and lake core sediments were examined by one-way nested ANOVA under generalized linear model (GLM) followed by post-hoc analysis (Tukey HSD (honest significant difference) test), and were performed with package 'car', 'carData' and 'agricolae'. Differences were considered to be significant at level of $p < 0.05$. To show how close our sample mean is close to the population mean, standard deviation is used (mean ± s.d.). To examine whether brGDGT signatures could distinguish soil OC derived from different land use types, principal component analysis (PCA) was performed with package 'FactoMineR' and 'factoextra'. The box plot and scatter plots were carried out with package 'ggplot2'.

3 Results

3.1 BrGDGTs in soils

Most of the brGDGTs were present in all soils. Only brGDGT–IIIc and brGDGT–IIIc' were always below the detection limit (peak height > 3x baseline), and brGDGT–IIc' was below the detection limit in 13 of the soils (three in arable land, four in grassland and six in ley). The brGDGTs were dominated by pentamethylated (49.4 ± 3.0%, mean ± s.d., standard deviation),

https://doi.org/10.5194/bg-2019-500
Preprint. Discussion started: 11 March 2020

175 followed by tetramethylated (39.7 ± 4.9%) and then hexamethylated brGDGTs (10.9 ± 2.6%; Table 1). The concentration of
176 brGDGTs ranged between 0.1 and 1.7 μg g^{-1} soil, with average of 0.2 ± 0.1 μg g^{-1} soil in arable land, 0.6 ± 0.4 μg g^{-1} soil in
177 grassland, and 0.4 ± 0.3 μg g^{-1} soil in ley (i.e. the temporary grassland). However, the concentration of brGDGTs in
178 woodland was 3.0 ± 1.0 μg g^{-1} soil, which was significantly higher than that in other land use types (0.4 ± 0.3 μg g^{-1} soil; $p <$
179 0.05; Fig. 3a). The C-normalized concentration of brGDGTs in catchment soils ranged between 2.8 to 49.8 μg g^{-1} C, 8.1 ±
180 3.6 μg g^{-1} C in arable land, 11.2 ± 6.7 μg g^{-1} C in grassland, 10.5 ± 4.8 μg g^{-1} C in ley, and 37.6 ± 11.0 μg g^{-1} C in woodland
181 (Fig. 3a; Table 1). The trend of the concentration of brGDGTs along the soil transects was not obvious.

182 BIT index values ranged from 0.57 to 1.00 among land use types (Fig. 3b), with an average value of 0.96 ± 0.03 in
183 woodland, 0.90 ± 0.12 in ley, 0.88 ± 0.14 in grassland and 0.83 ± 0.09 in arable land (without significant differences, $p >$
184 0.05). However, the BIT values increased from hillslope to downslope along several transects in north catchment, while the
185 BIT values show no clear trends in south catchment (Fig. A1). The MBT'$_{5ME}$ ranged from 0.37 to 0.71 and was mostly
186 similar between all land use types (0.48 ± 0.04; $p > 0.05$; Fig. 3c; Table 1). The degree of cyclization between land use types
187 was similar (DC = 0.23 ± 0.13; Fig. 3d; Table 1; $p > 0.05$), likewise, the IR ranged from 0.10 to 0.60 (0.28 ± 0.01 on
188 average; Fig. 3e; Table 1; $p > 0.05$), without clear trend along the soil transects. However, four transects in the north
189 catchment have on average significantly higher IR values (> 0.36) than the other transects in the catchment (0.24 ± 0.09; $p <$
190 0.05; Fig. A1). In general, the IR increases with increasing soil pH in the catchment ($r^2 = 0.36$, $p < 0.001$).

191 **3.2 BrGDGTs in creek bed sediments**

192 All brGDGT compounds were detected in creek bed sediments, except for in the upstream site from north catchment, where
193 brGDGT–IIIc' was below detection limit. The brGDGTs in creek bed sediments were dominated by pentamethylated
194 brGDGTs (45.0 ± 0.7%), followed by tetramethylated brGDGTs (30.1 ± 4.5%), and hexamethylated brGDGTs (24.9 ±
195 4.7%) (Table 1). The C-normalized concentration of brGDGTs in creek bed sediments was 34.7 ± 17.4 μg g^{-1} C on average
196 (Fig. 3a; Table 1), where the concentration increased from 32.7 μg g^{-1} C to 57.0 μg g^{-1} C downstream in north catchment,
197 and from 14.3 μg g^{-1} C to 25.2 μg g^{-1} C downstream in south catchment, reaching a maximum value of 59.3 μg g^{-1} C at the
198 outlet (Fig. 5a). The concentration of brGDGTs in creek bed sediments was higher than that in soils under any land use types
199 except for woodland (9.6 ± 4.9 μg g^{-1} C; Fig. 3a; Table 1).

200 The BIT values for creek sediments were on average 0.90 ± 0.06 (Fig. 3b; Table 1). The MBT'$_{5ME}$ was relatively constant
201 between 0.44 and 0.49, with an average of 0.46 ± 0.02. The DC ranged from 0.21 to 0.25 in the creek sediments with an
202 average of 0.23 ± 0.02 (Fig. 3e; Table 1). The IR was relatively invariable with an average of 0.48 ± 0.10 (Fig. 3e; Table 1).
203 The brGDGT-based indices in creek bed sediments were similar with the indices in soils, except for IR, which was higher
204 than that in soils under any land use types (0.28 ± 0.11; Fig. 3; Table 1).

https://doi.org/10.5194/bg-2019-500
Preprint. Discussion started: 11 March 2020


Biogeosciences Discussions Open Access EGU

3.3 BrGDGTs in Lake Loe Pool sediment core

All brGDGTs were detected in the lake sediment core, except at 20 cm depth, where brGDGT–IIIc' was below the detection limit. The brGDGTs in the lake sediments were mainly dominated by pentamethylated brGDGTs (50.2 ± 1.8%), followed by tetramethylated brGDGTs (28.9 ± 0.7%), and hexamethylated brGDGTs (21.0 ± 1.4%; Table 1). The amount of brGDGTs in lake core sediment ranged from 19.9 to 48.0 $\mu g\ g^{-1}$ C (Fig. 3a; Table 1). The brGDGT concentration in the surface sediment (0–2 cm), of 37.7 $\mu g\ g^{-1}$ C, which was about 1.6 times lower than that in the creek sediment at the outlet (Fig. 5a), increased to a maximum of 48.0 $\mu g\ g^{-1}$ C around 11 cm depth, and then decreased to a minimum of 19.9 $\mu g\ g^{-1}$ C at 23 cm depth (Fig. 6b). The concentration of GDGT-0 ranged between 9.0 $\mu g\ g^{-1}$ C and 27.1 $\mu g\ g^{-1}$ C with an average of 17.4 ± 6.0 $\mu g\ g^{-1}$ C, concentration of crenarchaeol ranged from 0.6 $\mu g\ g^{-1}$ C to 1.4 $\mu g\ g^{-1}$ C with an average of 1.0 ± 0.2 $\mu g\ g^{-1}$ C in the lake sediment core. In general, the concentration of brGDGTs in lake core (34.0 ± 8.7 $\mu g\ g^{-1}$ C; Table 1) was similar with that in river and in woodland, while it was significantly higher than the brGDGTs in soils except for the woodland (9.6 ± 4.9 $\mu g\ g^{-1}$ C; $p < 0.05$; Fig. 3a; Table 1).

The BIT values for the lake sediment core were rather uniform, varying between 0.95 and 0.97 (Fig.3b). Similarly, the values of MBT'_{5ME} along the lake core ranged only between 0.36 to 0.39. The MBT'_{5ME} of 0.37 for the lake surface sediment was significantly lower than that in creek bed sediment (0.46 ± 0.02; $p < 0.05$; Fig 3c; Fig. 5b). Conversely, the DC in the lake surface sediment was 0.39, which was significantly higher than that in creek bed sediment (0.23 ± 0.02; $p < 0.05$; Fig. 3d; Fig. 5b). The average value of DC for the lake core sediments was 0.32 ± 0.08. The DC increased from the surface to a maximum value (0.44) at around 10 cm depth, and then decreased with slight fluctuations to 0.22 at 43 cm depth (Fig. 6c). The IR was constant downcore (0.32 ± 0.01 on average; Fig. 3e; Table 1) and was significantly lower than that in creek bed sediment ($p < 0.05$; Fig. 3e).

4 Discussion

4.1 Spatial variation of brGDGT signals in catchment soils

Spatial variations in the relative distribution of brGDGTs in all catchment soils were first evaluated by performing principle component analysis (PCA) using the fractional abundances of the 13 major brGDGTs detected. The first two principal components (PCs) explain 65.2% of the variance in the dataset. PC1 describes 49.5% of the variance, and separates acyclic brGDGT–Ia and brGDGT–IIa from all the other brGDGTs (Fig. 4a). In line with this observation, PC1 has a strong positive relationship with the degree of cyclization of brGDGTs in the soils ($r^2 = 0.97$; Fig. 4c). PC2 describes another 15.7% of the variance, and separates tetramethylated brGDGTs as well as most of the 6-methyl brGDGTs from the majority of the 5-methyl penta- and hexamethylated brGDGTs. As a result, PC2 is negatively correlated with MBT'_{5ME} ($r^2 = 0.49$; Fig. 4d) as well as the IR ($r^2 = 0.58$; Fig. 4e) in soils. Despite the clear relation of the first two PCs with the degree of cyclization and

https://doi.org/10.5194/bg-2019-500
Preprint. Discussion started: 11 March 2020

235 the degree of methylation, respectively, the position of the soils in the PCA diagram reveals that different land use types are
236 largely overlapping (Fig. 4b). Indeed, the brGDGTs indices for different land use types are not significantly different ($p >$
237 0.05; Fig. 3), making it difficult to distinguish the provenance of soil OC solely based on brGDGT signatures.

238 Indeed, previous work has also shown that brGDGT distributions are not primarily affected by land use. For example,
239 brGDGTs in soils along an altitudinal transect in the Ethiopian highlands revealed that brGDGTs mainly reflect the decrease
240 in temperature with increasing elevation, regardless of drastic changes in land use along the transect (Jaeschke et al., 2018).
241 However, other studies report that vegetation cover does exert a great influence on brGDGT signatures in soils from
242 Minnesota and Ohio, USA (Weijers et al., 2011), around Lake Rotsee, Switzerland (Naeher et al., 2014), in the Tibetan
243 Plateau (Liang et al., 2019), and paddy and upland soils from subtropical (China and Italy) and tropical (Indonesia,
244 Philippines and Vietnam) areas (Mueller-Niggemann et al., 2016). The explanations for the similar distribution of brGDGTs
245 under different land use types in the Carminowe Creek catchment could be the rotation and ploughing in land use in
246 combination with the turnover time of brGDGTs. Although the soil bacterial community composition is generally different
247 across distinct land use types (Fierer & Jackson, 2006; Steenwerth et al., 2003), the regular rotation (generally less than 5
248 years) of arable land and temporary grassland (ley) in the catchment (Glendell et al., 2018) may create a mixed bacterial
249 community under all vegetation types. Beyond vegetation, regular ploughing as applied across the Carminowe catchment
250 soils (arable land and ley) is recognized to have a more dominant, long-last effect on microbial communities (Drenovsky et
251 al., 2010). Moreover, brGDGTs in soils have a relatively long turnover time of ca. 18 years (Weijers et al., 2010), especially
252 when compared to the cropland rotation time. These factors may contribute to the relatively similar brGDGT signal in all
253 soils in the Carminowe catchment, further limiting the variation in brGDGT signals in catchment soils.

254 Some spatial trends are visible in spite of the overall comparable brGDGT signals across the catchment (Fig. A1), which
255 may be explained by variations in other environmental factors than land use or vegetation. Mean air temperature and soil pH
256 have been shown to be the main factors controlling the distribution of brGDGTs in soils worldwide (Weijers et al., 2007a;
257 Peterse et al., 2012; De Jonge et al., 2014b). However, in the small (ca. 4.8 km^2) Carminowe Creek catchment, the annual
258 mean air temperature is practically the same for all soils. Similarly, the range in soil pH is relatively small among different
259 land use types (from 5.4 ± 0.3 in woodland to 6.6 ± 0.1 in arable land; Table 1), which makes it difficult to separate brGDGT
260 signals based on these parameters. Additionally, the soil water content (SWC) has been shown to affect the distribution and
261 abundance of brGDGTs in soils, either directly by changing the microbial community, or indirectly by altering soil
262 temperature, soil pH, or soil oxygen content (Dirghangi et al., 2013; Menges et al., 2014; Dang et al., 2016). The SWC
263 positively correlates with the abundance of brGDGTs in soils from Qinghai-Tibetan Plateau (Wang et al., 2013), as well as
264 in soils along an aridity transect in the USA (Dirghangi et al., 2013). Moreover, the degree of methylation of 6-methylated
265 brGDGTs is sensitive to the SWC, especially in semi-arid and arid regions (Dang et al., 2016). Although MAP is also the
266 same for the whole catchment, the subtle altitudinal differences in this small creek catchment (i.e. 0-80 m above sea level)

https://doi.org/10.5194/bg-2019-500
Preprint. Discussion started: 11 March 2020

may result in an increase in SWC from hilltop to downslope. This would introduce just enough variability in SWC to explain some of the trends in brGDGT signals along hillslope transects. In the north of the catchment, the BIT index values gradually increase > 0.4 from the presumably better aerated soils at the hilltops towards the wetter soils closer to the creek for two of the transects (Fig. A1). The change in BIT index values is driven by both an increase in the amount of brGDGTs and a slight decrease in crenarchaeol concentrations, similar to previous findings (Dirghangi et al., 2013; Wang et al., 2013; Menges et al., 2014). The trend in BIT is likely enhanced by the (minor) change in soil pH along these two transects (from 6.2 to 6.1 and from 6.6 to 5.7), which may influence the BIT index as a result of the generally positive relation of crenarchaeol concentrations and a negative relation of brGDGT concentrations with increasing soil pH (Weijers et al., 2006b; Peterse et al., 2010). Nevertheless, these trends in the BIT index are visible in only two of the hilltop transects in the north part of the catchment.

Interestingly, also the IR is significantly higher in soils along four transects in north catchment (> 0.36) compared to the average IR value for the rest of the catchment (0.24 ± 0.09; $p < 0.05$). The majority of the sites with higher IR are in cropland except for those in the Transect-1, which is under grassland (Fig. A2). Although a relative increase in 6-methyl brGDGTs has been linked to higher soil pH in the global soil dataset (De Jonge et al., 2014a), this relation is not so strong in the catchment soils ($r^2 = 0.36$, $p < 0.001$), likely due to the relatively minor range and variation in soil pH (from 5.4 ± 0.3 to 6.6 ± 0.1). Nevertheless, the soils with high IR values in the north catchment have pH values > 6.0 with an average value of 6.6 ± 0.1.

4.2 Tracing brGDGTs from soils to creek bed sediments

Based on the similar brGDGT signatures for soils under different land use types, these compounds cannot be used to trace back the exact source of the soil OC after mobilization and transport throughout the catchment. However, the concentration and general soil signature of the brGDGTs can be compared with those in creek bed sediments to trace the transfer of OC from the soils into the creeks. The C-normalized concentration of brGDGTs in the creek sediments is higher than that in most of the soils (34.7 ± 17.4 $\mu g\ g^{-1}$ C and 9.6 ± 4.9 $\mu g\ g^{-1}$ C respectively), except for those in the woodland soils at the riverbanks (37.6 ± 11.0 $\mu g\ g^{-1}$ C; Table 1). Thus, purely based on the concentration, this suggests that brGDGTs in the creek would be primarily derived from the woodland, which also appeared to be the main source of *n*-alkanes in creek bed sediment (Glendell et al., 2018). However, when looking at the relative distribution of the brGDGTs, the percentage of hexamethylated brGDGTs in creek sediments is higher than that in soils (24.9 ± 1.8% and 10.9 ± 0.3%, respectively), whereas the percentage of tetramethylated brGDGTs is lower than in soils (30.1 ± 1.7% and 39.7 ± 0.6%, respectively; Table 1). Furthermore, brGDGTs in creek sediments have a significantly higher IR (i.e. 0.48 ± 0.04) than soils under any of the land use types (0.28 ± 0.01 on average in the catchment; $p < 0.05$; Fig. 3e; Table 1). This is clearly reflected in the PCA, which separates the creek sediments from both the soils and lake sediments on PC2 that is associated with the IR (Fig. 4e). The higher IR in the creek bed sediments can be explained by a contribution of aquatically (i.e. *in situ*) produced 6-methyl

https://doi.org/10.5194/bg-2019-500
Preprint. Discussion started: 11 March 2020


Biogeosciences Discussions Open Access EGU

299 brGDGTs. Similar contributions of 6-methyl brGDGTs, and thus higher IR, were also observed in suspended particulate
300 matter from the Yenisei River (De Jonge et al., 2014a), and upstream of the Iron Gates in the Danube River, where the
301 higher IR was coupled to in-river production facilitated by the lower flow velocity and decreased turbidity of the river water
302 (Freymond et al., 2017). Hence, the significantly higher IR in combination with the higher C-normalized concentrations of
303 brGDGTs in the Carminowe creek sediments suggests that the brGDGT signal is mainly aquatic. This implies that the initial
304 soil brGDGT signal is rapidly overprinted by a riverine *in situ* signal upon entering the creek. Only the IR for the
305 downstream site in the northern creek approaches that of the adjacent soil (IR = 0.30 and 0.38 ± 0.02, respectively; Fig. A2),
306 and may be explained by its use as arable land (Fig. 5a), which involves regular ploughing and subsequent soil mobilization
307 and implies a temporary, local overprint.

308 In attempt to further prove the riverine *in situ* production of brGDGTs and explain the higher IR in creek bed sediment than
309 that in soils, we roughly estimate the minimum amount of 6-methyl brGDGTs produced in creek to reach the higher IR. We
310 assume that the brGDGTs derived from woodland are completely transferred into creek without any degradation, thus, the 6-
311 methyl brGDGTs in creek is composed by 6-methyl brGDGTs produced *in situ* ($6'_{Me\ in\ situ}$), which we are going to estimate
312 the exact values, and 6-methyl brGDGTs derived from woodland ($6'_{Me\ woodland}$). The minimum amount of 6-methyl
313 brGDGTs produced *in situ* was calculated based on the IR equation using absolute concentration of brGDGTs (Eq. 8).

314 $$IR_{concentration} = \frac{6'_{Me\ creek}}{5'_{Me\ creek} + 6'_{Me\ creek}} = \frac{6'_{Me\ woodland} + \mathbf{6'_{Me\ in\ situ}}}{5'_{Me\ creek} + 6'_{Me\ woodland} + \mathbf{6'_{Me\ in\ situ}}} \quad (8)$$

315 The minimum amount of riverine *in situ* 6-methyl brGDGTs production was 10.67 μg g^{-1} C, occupied 93.95% of the total
316 amount of 6-methyl brGDGTs in creek bed sediment we measured. Similarly, when considering the total soil transfer other
317 than only woodland, the minimum amount of riverine *in situ* 6-methyl brGDGTs was 10.66 μg g^{-1} C, accounting for 93.86%
318 of the total 6-methyl brGDGTs in creek bed sediment. It proves that the riverine *in situ* production of 6-methyl brGDGTs is
319 thriving.

320 The absence of a clearly recognizable soil brGDGT signal in the creek bed sediments may be explained by the relatively
321 limited input of soil material into the creek. So far, river systems that have shown to transport a soil-derived brGDGT signal
322 are either characterized by a rainy season (e.g. the Congo River; Weijers et al., 2007b; Hemingway et al., 2017), or have
323 experienced a recent episode of extreme rainfall (e.g. the Danube River, >100 mm in 3 days causing a 100-year flood event;
324 Freymond et al., 2017). The Carminowe creek area does not have a distinct rainy season, and is further characterized by its
325 limited relief. Hence, the relatively minor input of soil-derived brGDGTs seems to be easily overprinted by riverine *in situ*
326 production. Alternatively, the soil-derived brGDGTs are preferentially degraded in an aquatic environment, resulting in a
327 signature that is dominated by brGDGTs that are produced *in situ*.

https://doi.org/10.5194/bg-2019-500
Preprint. Discussion started: 11 March 2020


Biogeosciences Discussions Open Access EGU

4.3 Sources of brGDGTs in the sediments of Lake Loe Pool

In theory, rivers would transport soil-derived OC together with any aquatic OC produced along the way. Once discharged, in this case into a lake, the OC would settle and then be buried into the sediments where it would act as a long-term sink of OC. However, the soil brGDGT signal cannot be recognized in the sediments from Loe Pool since it is already lost upon entering the Carminowe creek. Indeed, the PCA of the relative distributions of brGDGTs indicates that lake sediments plot completely separated from both the soils and creek sediments, mostly due to a higher relative abundance of GDGT–IIIa (Fig. 4a, b). As a result, the MBT'_{5ME} is significantly lower in Loe Pool sediments (0.38 ± 0.00) compared to in the creek bed sediments (0.46 ± 0.01; $p < 0.05$) and soils (0.48 ± 0.01; $p < 0.05$; Fig. 5b; Table 1). Furthermore, the DC is significantly higher in lake sediments than in both soil and creek bed sediments (0.32 ± 0.02, 0.23 ± 0.01 and 0.23 ± 0.01, respectively; $p < 0.05$; Fig. 3d; Table 1). The distinct brGDGT signature of the lake sediments suggests that brGDGTs in the lake again are significantly altered compared to those in the soils and creek sediments. This implies that the riverine brGDGT signal is either replaced or overwritten in the lake.

Lacustrine *in situ* production of brGDGTs has been reported in other studies (Sinninghe Damsté et al., 2009a; Tierney and Russell, 2009; Loomis et al., 2011, 2014; Schoon et al., 2013; Weber et al., 2015, 2018). However, there are no generally recognized indicators (yet) to identify lacustrine brGDGT production, although several studies reported a "cold bias" while attempting to reconstruct the mean air temperature (MAT) based on brGDGTs in lake sediments using a soil-based transfer function (Tierney et al., 2010a). In a study on East African lakes, this cold bias was linked to a large *in situ* contribution of brGDGT–IIIa (Tierney et al., 2010a), similar to in Loe Pool. However, the East African lake dataset was generated using the 'old' chromatography method that does not separate 5-methyl and 6-methyl brGDGTs. A recent study that has re-analysed the East African Lake dataset indicates that the presumed contribution of GDGT–IIIa mainly consists of brGDGT–IIIa' (Russell et al., 2018), which is less prominent in lake Loe Pool. Although the identity of brGDGT-producer(s) in lakes still remain(s) elusive, a recent study from the stratified Lake Lugano (Switzerland) showed that brGDGTs are mostly produced in the lower, anoxic part of the water column rather than in the sediment (Weber et al., 2018). Furthermore, the combination of brGDGT analysis with molecular biological methods revealed that brGDGTs appeared to be produced by multiple groups of bacteria thriving under different redox regimes in this stratified lake. Specifically, brGDGT–IIIa occurred in the entire water column and continuously increased with depth, whereas brGDGT–IIIa' was mainly produced in the upper, oxygenated part of water column (Weber et al., 2018). Extrapolating the ecological niches of brGDGT production in Lake Lugano to Loe Pool we can speculate that brGDGT-IIIa, which is dominating the brGDGT signal in the Loe Pool sediments, is mostly produced in summer, when the eutrophic state of the lake may seasonally cause the anoxic conditions favourable for its (i.e. brGDGT-IIIa) production. However, our dataset does not allow to further pinpoint the time and depth of lacustrine brGDGT production, or whether brGDGTs are solely produced in the water column of Loe Pool or also in the lake sediment.

https://doi.org/10.5194/bg-2019-500
Preprint. Discussion started: 11 March 2020

4.4 Reconstructing local environmental changes based on GDGTs in Loe Pool lake sediments

Downcore variations in the brGDGT distribution of Lake Pool sediments may provide information on past environmental changes in the catchment, in spite of the lacustrine *in situ* production in Lake Loe Pool. The 50 cm deep sediment core covers about the last 100 years based on ^{137}Cs activity (Glendell et al., 2018). The peak activity correlated with bomb testing in the 1960s was detected at 26 cm depth (Fig. 6a), which can thus be linked to 1963 (Glendell et al., 2018).

The C-normalized concentration of brGDGTs starts to increase around 23 cm, reaching a maximum concentration of 48.0 $\mu g\ g^{-1}$ C at 11 cm depth (Fig. 6b). The increased brGDGT concentrations coincide with an increase in the degree of cyclization (Fig. 6c), which generally responds to a change in pH, where more cyclopentane moieties correspond to a higher pH (Weijers et al., 2007a; Schoon et al., 2013). According to historical records, agriculture and anthropogenic perturbations such as mining and urban pollution intensified in the 1960s (~ 26 cm depth), which increased the input of soil and nutrients into Lake Loe Pool (Coard et al., 1983), and resulted in eutrophication (i.e. blooms of cyanobacteria and algae) since at least 1986 (~ 23 cm depth) (O'Sullivan, 1992; Flory and Hawley, 1994). Earlier studies have also recognized an increased use of farmyard manures and septic tanks at this time in the nitrogen isotopic composition of the lake sediments, and have detected higher inputs of terrestrial organic material resulting from intensified farming practices and a higher erosion rate during the 1960s to 1980s based on ratios of aquatic- and terrestrial-derived plant waxes (Glendell et al., 2018). Thus, the high brGDGT concentrations and DC in the sediments likely reflect the eutrophic conditions of the lake resulting from the increased nutrient input to the lake (Coard et al., 1983). The DC has then recorded the increase in lake water pH associated with eutrophication, whereas brGDGT concentrations express increased aquatic production. Due to remediation measures taken by the local government in 1996 (~ 12 cm depth), the eutrophication has reduced over the past twenty years (Flory and Hawley, 1994; Glendell et al., 2018). The partial recovery of the lake has likely resulted in a return to lower lake water pH, as manifested in the decrease in the DC from ~ 10 cm depth upwards (Fig. 6c).

The process of eutrophication and subsequent recovery can also be recognized in the ratio between GDGT–0 and crenarchaeol, which are isoprenoidal GDGTs produced by Archaea. Crenarchaeol is produced by ammonia oxidizing Thaumarchaeota (Sinninghe Damsté et al., 2002) in aquatic environments (Schouten et al., 2000; Powers et al., 2004) and to a lesser extent also in soils (Weijers et al., 2006a), whereas GDGT–0 is a membrane lipid that occurs in all major groups of Archaea, but is indicative of methanogens and thus anaerobic conditions, with a typical ratio of GDGT-0 and crenarchaeol > 2 (Blaga et al., 2009). The ratio of GDGT-0/crenarchaeol in the sediments of Loe Pool is > 2 throughout the entire core, and ranges between 10.9 and 24.3, indicating that at least the bottom waters of the lake have been (seasonally) anoxic over the past 100 years (Fig. 6d). The ratio reaches its maximum at 16 cm depth, suggesting that eutrophic conditions and bottom water anoxia were most severe around this time. The recovery of the lake after the remediation measures is again reflected in the return to pre-1960 values (Fig. 6d).

https://doi.org/10.5194/bg-2019-500
Preprint. Discussion started: 11 March 2020

5 Conclusions

In this study, brGDGTs were tested as a tracer for the transport of soil OC from different vegetation and land use types from source (soil) to sink (lake Loe Pool) in the Carminowe Creek catchment with the aim to reconstruct the provenance of the soil OC in lake Loe Pool sediments over time. Unfortunately, brGDGT signatures in the catchment soils are not distinct for land use types, indicating that other environmental parameters have a larger influence on the distribution of brGDGTs in these soils. Although temperature and precipitation can be considered equal for all soils due to the small size of the catchment, changes in BIT index values and the relative contribution of 6-methyl brGDGTs along a part of the hilltop transects indicate that soil water content (SWC) likely exerts a control on brGDGT signals, assuming that SWC increases downslope. The regular rotation of cropland in this catchment and the relative long turnover time of brGDGTs in soils could be another reason to explain the limited spatial variation in brGDGT signals.

Comparison of the soil-derived brGDGT signals to that of creek bed sediments reveals that the soil brGDGT signal is replaced by aquatically produced brGDGTs, indicated by a substantially higher fractional abundance of 6-methyl brGDGTs in the creek. Upon discharge into the lake, the creek brGDGT signal is replaced by a lacustrine *in situ* produced brGDGT signal, which is characterized by a relatively higher DC and lower MBT'_{5ME}, as well as a specifically high fractional abundance brGDGT-IIIa. Despite regular ploughing of the land, the absence of a profound rainy season and limited relief likely limits the degree of soil mobilization necessary to transfer the soil-derived brGDGT signal to the lake sediments in the modern system. Still, downcore variations in GDGT distributions in the sediments of Loe Pool do reflect local environmental conditions over the past 100 years. The weighed degree of cyclization of brGDGTs as well as the ratio of isoprenoidal GDGT-0 and crenarchaeol produced by Archaea match well with the historical record of lake eutrophication induced by increased nutrient input from intensified agricultural activity in the catchment during the 1960s to 1980s, and its recovery after measures taken by the owner since 1996. Our study shows that GDGTs in sedimentary archives are good recorders of past environmental and land management change, although the ability of brGDGTs to trace soil OC along a soil-aquatic continuum requires a higher degree of soil mobilization.

Data availability

All data are available in the Supplementary Information.

Author Contribution

J.M., F.K., and F.P designed the study, M.G. and J.M. collected the sample material. J.G. conducted the biomarker analysis and interpreted the data under supervision of F.P. and J.J.M, J.G. and F.P wrote the paper with input from all co-authors.

https://doi.org/10.5194/bg-2019-500
Preprint. Discussion started: 11 March 2020

418 **Competing interests**

419 The authors declare that they have no conflict of interest.

420 **Acknowledgements**

421 This study was supported financially by NWO Veni grant #863.13.016 to Francien Peterse. Desmond Eefting and Klaas
422 Nierop are acknowledged for technical support.

423 **References**

424 Aufdenkampe, A. K., Mayorga, E., Raymond, P. A., Melack, J. M., Doney, S. C., Alin, S. R., Aalto, R. E. and Yoo, K.:
425 Riverine coupling of biogeochemical cycles between land, oceans, and atmosphere, Front. Ecol. Environ., 9(1), 53–60,
426 doi:10.1890/100014, 2011.
427 Battin, T. J., Luyssaert, S., Kaplan, L. A., Aufdenkampe, A. K., Richter, A. and Tranvik, L. J.: The boundless carbon cycle,
428 Nat. Geosci., 2(9), 598–600, doi:10.1038/ngeo618, 2009.
429 Baxter, A. J., Hopmans, E. C. and Russell, J. M.: ScienceDirect Bacterial GMGTs in East African lake sediments : Their
430 potential as palaeotemperature indicators, , 259, 155–169, doi:10.1016/j.gca.2019.05.039, 2019.
431 Bianchi, T. S., Filley, T., Dria, K. and Hatcher, P. G.: Temporal variability in sources of dissolved organic carbon in the
432 lower Mississippi River, Geochim. Cosmochim. Acta, 68(5), 959–967, doi:10.1016/j.gca.2003.07.011, 2004.
433 Blaga, C. I., Reichart, G. J., Heiri, O. and Sinninghe Damsté, J. S.: Tetraether membrane lipid distributions in water-column
434 particulate matter and sediments: A study of 47 European lakes along a north-south transect, J. Paleolimnol., 41(3), 523–540,
435 doi:10.1007/s10933-008-9242-2, 2009.
436 Blair, N. E., Leithold, E. L. and Aller, R. C.: From bedrock to burial: the evolution of particulate organic carbon across
437 coupled watershed-continental margin systems, Mar. Chem., 92(1–4), 141–156, doi:10.1016/j.marchem.2004.06.023, 2004.
438 Brassell, S. C. and Eglinton, G.: Molecular Geochemical Indicators in Sediments, edited by M. L. Sohn, pp. 10–32,
439 Washington, D.C., 1986.
440 Coard, M. A., Cousen, S. M., Cuttler, A. H., Dean, H. J., Dearing, J. A., Eglinton, T. I., Greaves, A. M., Lacey, K. P.,
441 O'Sullivan, P. E., Pickering, D. A., Rhead, M. M., Rodwell, J. K. and Simola, H.: Paleolimnological studies of annually-
442 laminated sediments in Loe Pool, Cornwall, U.K., Hydrobiologia, 103(1), 185–191, doi:10.1007/BF00028450, 1983.
443 Cole, J. J., Prairie, Y. T., Caraco, N. F., McDowell, W. H., Tranvik, L. J., Striegl, R. G., Duarte, C. M., Kortelainen, P.,
444 Downing, J. A., Middelburg, J. J. and Melack, J.: Plumbing the global carbon cycle: Integrating inland waters into the
445 terrestrial carbon budget, Ecosystems, 10(1), 171–184, doi:10.1007/s10021-006-9013-8, 2007.
446 Dang, X., Yang, H., Naafs, B. D. A., Pancost, R. D. and Xie, S.: Evidence of moisture control on the methylation of
447 branched glycerol dialkyl glycerol tetraethers in semi-arid and arid soils, Geochim. Cosmochim. Acta, 189, 24–36,

https://doi.org/10.5194/bg-2019-500
Preprint. Discussion started: 11 March 2020

448 doi:10.1016/j.gca.2016.06.004, 2016.
449 Davidson, E. A. and Janssens, I. A.: Temperature sensitivity of soil carbon decomposition and feedbacks to climate change,
450 Nature, 440(7081), 165–173, doi:10.1038/nature04514, 2006.
451 Dearing Crampton-Flood, E., Peterse, F., Munsterman, D. and Sinninghe Damsté, J. S.: Using tetraether lipids archived in
452 North Sea Basin sediments to extract North Western European Pliocene continental air temperatures, Earth Planet. Sci. Lett.,
453 490(March), 193–205, doi:10.1016/j.epsl.2018.03.030, 2018.
454 De Jonge, C., Hopmans, E. C., Stadnitskaia, A., Rijpstra, W. I. C., Hofland, R., Tegelaar, E. and Sinninghe Damsté, J. S.:
455 Identification of novel penta- and hexamethylated branched glycerol dialkyl glycerol tetraethers in peat using HPLC–MS2,
456 GC–MS and GC–SMB-MS, Org. Geochem., 54, 78–82, doi:10.1016/j.orggeochem.2012.10.004, 2013.
457 De Jonge, C., Stadnitskaia, A., Hopmans, E. C., Cherkashov, G., Fedotov, A. and Sinninghe Damsté, J. S.: In situ produced
458 branched glycerol dialkyl glycerol tetraethers in suspended particulate matter from the Yenisei River, Eastern Siberia,
459 Geochim. Cosmochim. Acta, 125, 476–491, doi:10.1016/j.gca.2013.10.031, 2014a.
460 De Jonge, C., Hopmans, E. C., Zell, C. I., Kim, J.-H., Schouten, S. and Sinninghe Damsté, J. S.: Occurrence and abundance
461 of 6-methyl branched glycerol dialkyl glycerol tetraethers in soils: Implications for palaeoclimate reconstruction, Geochim.
462 Cosmochim. Acta, 141, 97–112, doi:10.1016/j.gca.2014.06.013, 2014b.
463 Dirghangi, S. S., Pagani, M., Hren, M. T. and Tipple, B. J.: Distribution of glycerol dialkyl glycerol tetraethers in soils from
464 two environmental transects in the USA, Org. Geochem., 59, 49–60, doi:10.1016/j.orggeochem.2013.03.009, 2013a.
465 Dirghangi, S. S., Pagani, M., Hren, M. T. and Tipple, B. J.: Distribution of glycerol dialkyl glycerol tetraethers in soils from
466 two environmental transects in the USA, Org. Geochem., 59, 49–60, doi:10.1016/j.orggeochem.2013.03.009, 2013b.
467 Drenovsky, R. E., Steenwerth, K. L., Jackson, L. E. and Scow, K. M.: Land use and climatic factors structure regional
468 patterns in soil microbial communities, Glob. Ecol. Biogeogr., 19(1), 27–39, doi:10.1111/j.1466-8238.2009.00486.x, 2010.
469 Eglinton, G. and Hamilton, R. J.: Leaf Epicuticular Waxes, Science (80-.)., 156(3780), 1322–1335,
470 doi:10.1126/science.156.3780.1322, 1967.
471 Feng, X., Vonk, J. E., van Dongen, B. E., Gustafsson, O., Semiletov, I. P., Dudarev, O. V., Wang, Z., Montlucon, D. B.,
472 Wacker, L. and Eglinton, T. I.: Differential mobilization of terrestrial carbon pools in Eurasian Arctic river basins, Proc.
473 Natl. Acad. Sci., 110(35), 14168–14173, doi:10.1073/pnas.1307031110, 2013.
474 Feng, X., Feakins, S. J., Liu, Z., Ponton, C., Wang, R. Z., Karkabi, E., Galy, V., Berelson, W. M., Nottingham, A. T., Meir,
475 P. and West, A. J.: Source to sink: Evolution of lignin composition in the Madre de Dios River system with connection to the
476 Amazon basin and offshore, J. Geophys. Res. Biogeosciences, 121(5), 1316–1338, doi:10.1002/2016JG003323, 2016.
477 Fernandes, M. B. and Sicre, M. A.: The importance of terrestrial organic carbon inputs on Kara Sea shelves as revealed by n-
478 alkanes, OC and δ13C values, Org. Geochem., 31(5), 363–374, doi:10.1016/S0146-6380(00)00006-1, 2000.
479 Fierer, N. and Jackson, R. B.: The diversity and biogeography of soil bacterial communities., Proc. Natl. Acad. Sci. U. S. A.,
480 103(3), 626–31, doi:10.1073/pnas.0507535103, 2006.
481 Flory, J. E. and Hawley, G. R. W.: A hydrodictyon reticulatum bloom at loe pool, cornwall, Eur. J. Phycol., 29(1), 17–20,

482 doi:10.1080/09670269400650431, 1994.
483 Freymond, C. V., Peterse, F., Fischer, L. V., Filip, F., Giosan, L. and Eglinton, T. I.: Branched GDGT signals in fluvial
484 sediments of the Danube River basin: Method comparison and longitudinal evolution, Org. Geochem., 103, 88–96,
485 doi:10.1016/j.orggeochem.2016.11.002, 2017.
486 Glendell, M., Jones, R., Dungait, J. A. J., Meusburger, K., Schwendel, A. C., Barclay, R., Barker, S., Haley, S., Quine, T. A.
487 and Meersmans, J.: Tracing of particulate organic C sources across the terrestrial-aquatic continuum, a case study at the
488 catchment scale (Carminowe Creek, southwest England), Sci. Total Environ., 616–617, 1077–1088,
489 doi:10.1016/j.scitotenv.2017.10.211, 2018.
490 Goñi, M. A., Ruttenberg, K. C. and Eglinton, T. I.: Sources and contribution of terrigenous organic carbon to surface
491 sediments in the Gulf of Mexico, Nature, 389(6648), 275–278, doi:10.1038/38477, 1997.
492 Hedges, J. I., Clark, W. A., Quay, P. D., Richey, J. E., Devol, A. H. and Santos, M.: Compositions and fluxes of particulate
493 organic material in the Amazon River, Limnol. Oceanogr., 31(4), 717–738, doi:10.4319/lo.1986.31.4.0717, 1986.
494 Hedges, J. I., Keil, R. G. and Benner, R.: What happens to terrestrial organic matter in the ocean?, Org. Geochem., 27(5–6),
495 195–212, doi:10.1016/S0146-6380(97)00066-1, 1997.
496 Hedges, J. I., Mayorga, E., Tsamakis, E., McClain, M. E., Aufdenkampe, A., Quay, P., Richey, J. E., Benner, R., Opsahl, S.,
497 Black, B., Pimentel, T., Quintanilla, J. and Maurice, L.: Organic matter in Bolivian tributaries of the Amazon River: A
498 comparison to the lower mainstream, Limnol. Oceanogr., 45(7), 1449–1466, doi:10.4319/lo.2000.45.7.1449, 2000.
499 Hemingway, J. D., Schefuß, E., Spencer, R. G. M., Dinga, B. J., Eglinton, T. I., McIntyre, C. and Galy, V. V.: Hydrologic
500 controls on seasonal and inter-annual variability of Congo River particulate organic matter source and reservoir age, Chem.
501 Geol., 466(October), 454–465, doi:10.1016/j.chemgeo.2017.06.034, 2017.
502 Hopmans, E. C., Weijers, J. W. H., Schefuß, E., Herfort, L., Sinninghe Damsté, J. S. and Schouten, S.: A novel proxy for
503 terrestrial organic matter in sediments based on branched and isoprenoid tetraether lipids, Earth Planet. Sci. Lett., 224(1–2),
504 107–116, doi:10.1016/j.epsl.2004.05.012, 2004.
505 Hopmans, E. C., Schouten, S. and Sinninghe Damsté, J. S.: The effect of improved chromatography on GDGT-based
506 palaeoproxies, Org. Geochem., 93, 1–6, doi:10.1016/j.orggeochem.2015.12.006, 2016.
507 Huguet, C., Hopmans, E. C., Febo-Ayala, W., Thompson, D. H., Sinninghe Damsté, J. S. and Schouten, S.: An improved
508 method to determine the absolute abundance of glycerol dibiphytanyl glycerol tetraether lipids, Org. Geochem., 37(9), 1036–
509 1041, doi:10.1016/j.orggeochem.2006.05.008, 2006.
510 Inglis, G. N., Collinson, M. E., Riegel, W., Wilde, V., Farnsworth, A., Lunt, D. J., Valdes, P., Robson, B. E., Scott, A. C.,
511 Lenz, O. K., Naafs, B. D. A. and Pancost, R. D.: Mid-latitude continental temperatures through the early Eocene in western
512 Europe, Earth Planet. Sci. Lett., 460, 86–96, doi:10.1016/j.epsl.2016.12.009, 2017.
513 Jaeschke, A., Rethemeyer, J., Lappé, M., Schouten, S., Boeckx, P. and Schefuß, E.: Influence of land use on distribution of
514 soil n-alkane δD and brGDGTs along an altitudinal transect in Ethiopia: Implications for (paleo)environmental studies, Org.
515 Geochem., 124, 77–87, doi:10.1016/j.orggeochem.2018.06.006, 2018.

https://doi.org/10.5194/bg-2019-500
Preprint. Discussion started: 11 March 2020

516 Janzen, H. H.: Carbon cycling in earth systems - A soil science perspective, Agric. Ecosyst. Environ., 104(3), 399–417,
517 doi:10.1016/j.agee.2004.01.040, 2004.
518 Liang, J., Russell, J. M., Xie, H., Lupien, R. L., Si, G., Wang, J., Hou, J. and Zhang, G.: Vegetation effects on temperature
519 calibrations of branched glycerol dialkyl glycerol tetraether (brGDGTs) in soils, Org. Geochem., 127, 1–11,
520 doi:10.1016/j.orggeochem.2018.10.010, 2019.
521 Loomis, S. E., Russell, J. M. and Sinninghe Damsté, J. S.: Distributions of branched GDGTs in soils and lake sediments
522 from western Uganda: Implications for a lacustrine paleothermometer, Org. Geochem., 42(7), 739–751,
523 doi:10.1016/j.orggeochem.2011.06.004, 2011.
524 Loomis, S. E., Russell, J. M., Heureux, A. M., D'Andrea, W. J. and Sinninghe Damsté, J. S.: Seasonal variability of
525 branched glycerol dialkyl glycerol tetraethers (brGDGTs) in a temperate lake system, Geochim. Cosmochim. Acta, 144,
526 173–187, doi:10.1016/j.gca.2014.08.027, 2014.
527 Menges, J., Huguet, C., Alcañiz, J. M., Fietz, S., Sachse, D. and Rosell-Melé, A.: Influence of water availability in the
528 distributions of branched glycerol dialkyl glycerol tetraether in soils of the Iberian Peninsula, Biogeosciences, 11(10), 2571–
529 2581, doi:10.5194/bg-11-2571-2014, 2014.
530 Ménot, G., Bard, E., Rostek, F., Weijers, J. W. H., Hopmans, E. C., Schouten, S. and Sinninghe Damsté, J. S.: Early
531 Reactivation of European Rivers During the Last Deglaciation, Science (80-.)., 313(September), 1623–1625, 2006.
532 Mueller-Niggemann, C., Utami, S. R., Marxen, A., Mangelsdorf, K., Bauersachs, T. and Schwark, L.: Distribution of
533 tetraether lipids in agricultural soils – differentiation between paddy and upland management,
534 Biogeosciences, 13(5), 1647–1666, doi:10.5194/bg-13-1647-2016, 2016.
535 Naafs, B. D. A., Inglis, G. N., Zheng, Y., Amesbury, M. J., Biester, H., Bindler, R., Blewett, J., Burrows, M. A., del Castillo
536 Torres, D., Chambers, F. M., Cohen, A. D., Evershed, R. P., Feakins, S. J., Gałka, M., Gallego-Sala, A., Gandois, L., Gray,
537 D. M., Hatcher, P. G., Honorio Coronado, E. N., Hughes, P. D. M., Huguet, A., Könönen, M., Laggoun-Défarge, F.,
538 Lähteenoja, O., Lamentowicz, M., Marchant, R., McClymont, E., Pontevedra-Pombal, X., Ponton, C., Pourmand, A.,
539 Rizzuti, A. M., Rochefort, L., Schellekens, J., De Vleeschouwer, F. and Pancost, R. D.: Introducing global peat-specific
540 temperature and pH calibrations based on brGDGT bacterial lipids, Geochim. Cosmochim. Acta, 208(June 2016), 285–301,
541 doi:10.1016/j.gca.2017.01.038, 2017.
542 Naeher, S., Peterse, F., Smittenberg, R. H., Niemann, H., Zigah, P. K. and Schubert, C. J.: Sources of glycerol dialkyl
543 glycerol tetraethers (GDGTs) in catchment soils, water column and sediments of Lake Rotsee (Switzerland) - Implications
544 for the application of GDGT-based proxies for lakes, Org. Geochem., 66, 164–173, doi:10.1016/j.orggeochem.2013.10.017,
545 2014.
546 O'Sullivan, P. E.: The eutrophication of shallow coastal lakes inn Southwest Enngland- unnderstanndinng and
547 recommendations for restoration, based on paleolimnology, historical records, and the modellinng of changing phosphorus
548 loads. Hydrobiologia, 243(1), 421-434, doi.org/10.1007/BF00007059, 1992.
549 Peterse, F., Kim, J. H., Schouten, S., Kristensen, D. K., Koç, N. and Sinninghe Damsté, J. S.: Constraints on the application

of the MBT/CBT palaeothermometer at high latitude environments (Svalbard, Norway), Org. Geochem., 40(6), 692–699, doi:10.1016/j.orggeochem.2009.03.004, 2009.

Peterse, F., Nicol, G. W., Schouten, S. and Sinninghe Damsté, J. S.: Influence of soil pH on the abundance and distribution of core and intact polar lipid-derived branched GDGTs in soil, Org. Geochem., 41(10), 1171–1175, doi:10.1016/j.orggeochem.2010.07.004, 2010.

Peterse, F., Prins, M. A., Beets, C. J., Troelstra, S. R., Zheng, H., Gu, Z., Schouten, S. and Damsté, J. S. S.: Decoupled warming and monsoon precipitation in East Asia over the last deglaciation, Earth Planet. Sci. Lett., 301(1–2), 256–264, doi:10.1016/j.epsl.2010.11.010, 2011.

Peterse, F., van der Meer, J., Schouten, S., Weijers, J. W. H., Fierer, N., Jackson, R. B., Kim, J. H. and Sinninghe Damsté, J. S.: Revised calibration of the MBT-CBT paleotemperature proxy based on branched tetraether membrane lipids in surface soils, Geochim. Cosmochim. Acta, 96, 215–229, doi:10.1016/j.gca.2012.08.011, 2012.

Powers, L. A., Werne, J. P., Johnson, T. C., Hopmans, E. C., Sinninghe Damsté, J. S. and Schouten, S.: Crenarchaeotal membrane lipids in lake sediments: A new paleotemperature proxy continental paleoclimate reconstruction?, Geology, 32(7), 613–616, doi:10.1130/G20434.1, 2004.

R Code Team, R: A language and environment for statistical computing, http://www.R-project.org, 2018.

Russell, J. M., Hopmans, E. C., Loomis, S. E., Liang, J. and Sinninghe Damsté, J. S.: Distributions of 5- and 6-methyl branched glycerol dialkyl glycerol tetraethers (brGDGTs) in East African lake sediment: Effects of temperature, pH, and new lacustrine paleotemperature calibrations, Org. Geochem., 117, 56–69, doi:10.1016/j.orggeochem.2017.12.003, 2018.

Schoon, P. L., De Kluijver, A., Middelburg, J. J., Downing, J. A., Sinninghe Damsté, J. S. and Schouten, S.: Influence of lake water pH and alkalinity on the distribution of core and intact polar branched glycerol dialkyl glycerol tetraethers (GDGTs) in lakes, Org. Geochem., 60, 72–82, doi:10.1016/j.orggeochem.2013.04.015, 2013.

Schouten, S., Hopmans, E. C., Pancost, R. D. and Sinninghe Damsté, J. S.: Widespread occurrence of structurally diverse tetraether membrane lipids: Evidence for the ubiquitous presence of low-temperature relatives of hyperthermophiles, Proc. Natl. Acad. Sci., 97(26), 14421–14426, doi:10.1073/pnas.97.26.14421, 2000.

Sinninghe Damsté, J. S., Schouten, S., Hopmans, E. C., van Duin, A. C. T. and Geenevasen, J. A. J.: Crenarchaeol, J. Lipid Res., 43(10), 1641–1651, doi:10.1194/jlr.M200148-JLR200, 2002.

Sinninghe Damsté, J. S., Ossebaar, J., Abbas, B., Schouten, S. and Verschuren, D.: Fluxes and distribution of tetraether lipids in an equatorial African lake: Constraints on the application of the TEX86 palaeothermometer and BIT index in lacustrine settings, Geochim. Cosmochim. Acta, 73(14), 4232–4249, doi:10.1016/j.gca.2009.04.022, 2009.

Sinninghe Damsté, J. S., Rijpstra, W. I. C., Hopmans, E. C., Weijers, J. W. H., Foesel, B. U., Overmann, J. and Dedysh, S. N.: 13,16-Dimethyl octacosanedioic acid (iso-Diabolic Acid), a common membrane-spanning lipid of Acidobacteria subdivisions 1 and 3, Appl. Environ. Microbiol., 77(12), 4147–4154, doi:10.1128/AEM.00466-11, 2011.

Sinninghe Damsté, J. S., Rijpstra, W. I. C., Hopmans, E. C., Foesel, B. U., Wüst, P. K., Overmann, J., Tank, M., Bryant, D. A., Dunfield, P. F., Houghton, K. and Stott, M. B.: Ether- and ester-bound iso-diabolic acid and other lipids in members of

https://doi.org/10.5194/bg-2019-500
Preprint. Discussion started: 11 March 2020

584 Acidobacteria subdivision 4, Appl. Environ. Microbiol., 80(17), 5207–5218, doi:10.1128/AEM.01066-14, 2014.
585 Sinninghe Damsté, J. S.: Spatial heterogeneity of sources of branched tetraethers in shelf systems: The geochemistry of
586 tetraethers in the Berau River delta (Kalimantan, Indonesia), Geochim. Cosmochim. Acta, 186, 13–31,
587 doi:10.1016/j.gca.2016.04.033, 2016.
588 Sinninghe Damsté, J. S., Rijpstra, W. I. C., Foesel, B. U., Huber, K. J., Overmann, J., Nakagawa, S., Kim, J. J., Dunfield, P.
589 F., Dedysh, S. N. and Villanueva, L.: An overview of the occurrence of ether- and ester-linked iso-diabolic acid membrane
590 lipids in microbial cultures of the Acidobacteria: Implications for brGDGT paleoproxies for temperature and pH, Org.
591 Geochem., 124, 63–76, doi:10.1016/j.orggeochem.2018.07.006, 2018.
592 Smith, P.: Land use change and soil organic carbon dynamics, Nutr. Cycl. Agroecosystems, 81(2), 169–178,
593 doi:10.1007/s10705-007-9138-y, 2008.
594 Steenwerth, K. L., Jackson, L. E., Calderón, F. J., Stromberg, M. R. and Scow, K. M.: Erratum: Soil community composition
595 and land use history in cultivated and grassland ecosystems of coastal California (Soil Biology and Biochemistry 34:11
596 (1599-1611)), Soil Biol. Biochem., 35(3), 487–500, doi:10.1016/S0038-0717(03)00027-0, 2003.
597 Tierney, J. E. and Russell, J. M.: Distributions of branched GDGTs in a tropical lake system: Implications for lacustrine
598 application of the MBT/CBT paleoproxy, Org. Geochem., 40(9), 1032–1036, doi:10.1016/j.orggeochem.2009.04.014, 2009.
599 Tierney, J. E., Russell, J. M., Eggermont, H., Hopmans, E. C., Verschuren, D. and Sinninghe Damsté, J. S.: Environmental
600 controls on branched tetraether lipid distributions in tropical East African lake sediments, Geochim. Cosmochim. Acta,
601 74(17), 4902–4918, doi:10.1016/j.gca.2010.06.002, 2010.
602 Wakeham, S. G. and Lee, C.: Organic Geochemistry, edited by M. H. Engel and S. A. Macko, Springer US, Boston, MA.,
603 1993.
604 Wang, H., Liu, W., Zhang, C. L., Liu, Z. and He, Y.: Branched and isoprenoid tetraether (BIT) index traces water content
605 along two marsh-soil transects surrounding Lake Qinghai: Implications for paleo-humidity variation, Org. Geochem., 59,
606 75–81, doi:10.1016/j.orggeochem.2013.03.011, 2013.
607 Weber, Y., De Jonge, C., Rijpstra, W. I. C., Hopmans, E. C., Stadnitskaia, A., Schubert, C. J., Lehmann, M. F., Sinninghe
608 Damsté, J. S. and Niemann, H.: Identification and carbon isotope composition of a novel branched GDGT isomer in lake
609 sediments: Evidence for lacustrine branched GDGT production, Geochim. Cosmochim. Acta, 154, 118–129,
610 doi:10.1016/j.gca.2015.01.032, 2015.
611 Weber, Y., Sinninghe Damsté, J. S., Zopfi, J., De Jonge, C., Gilli, A., Schubert, C. J., Lepori, F., Lehmann, M. F. and
612 Niemann, H.: Redox-dependent niche differentiation provides evidence for multiple bacterial sources of glycerol tetraether
613 lipids in lakes, Proc. Natl. Acad. Sci., 115(43), 10926–10931, doi:10.1073/pnas.1805186115, 2018.
614 Weijers, J. W. H., Schouten, S., Hopmans, E. C., Geenevasen, J. A. J., David, O. R. P., Coleman, J. M., Pancost, R. D. and
615 Sinninghe Damste, J. S.: Membrane lipids of mesophilic anaerobic bacteria thriving in peats have typical archaeal traits,
616 Environ. Microbiol., 8(4), 648–657, doi:10.1111/j.1462-2920.2005.00941.x, 2006a.
617 Weijers, J. W. H., Schouten, S., Spaargaren, O. C. and Sinninghe Damsté, J. S.: Occurrence and distribution of tetraether

618 membrane lipids in soils: Implications for the use of the TEX86 proxy and the BIT index, Org. Geochem., 37(12), 1680–
619 1693, doi:10.1016/j.orggeochem.2006.07.018, 2006b.
620 Weijers, J. W. H., Schouten, S., van den Donker, J. C., Hopmans, E. C. and Sinninghe Damsté, J. S.: Environmental controls
621 on bacterial tetraether membrane lipid distribution in soils, Geochim. Cosmochim. Acta, 71(3), 703–713,
622 doi:10.1016/j.gca.2006.10.003, 2007a.
623 Weijers, J. W. H., Schefuß, E., Schouten, S. and Sinninghe Damsté, J. S.: Evolution of Tropical Africa over the Last
624 Deglaciation, Science (80-.)., 8247(March), 5–8, 2007b.
625 Weijers, J. W. H., Wiesenberg, G. L. B., Bol, R., Hopmans, E. C. and Pancost, R. D.: Carbon isotopic composition of
626 branched tetraether membrane lipids in soils suggest a rapid turnover and a heterotrophic life style of their source
627 organism(s), Biogeosciences, 7(9), 2959–2973, doi:10.5194/bg-7-2959-2010, 2010.
628 Weijers, J. W. H., Bernhardt, B., Peterse, F., Werne, J. P., Dungait, J. A. J., Schouten, S. and Sinninghe Damsté, J. S.:
629 Absence of seasonal patterns in MBT-CBT indices in mid-latitude soils, Geochim. Cosmochim. Acta, 75(11), 3179–3190,
630 doi:10.1016/j.gca.2011.03.015, 2011.
631 Zell, C., Kim, J. H., Moreira-Turcq, P., Abril, G., Hopmans, E. C., Bonnet, M. P., Sobrinho, R. L. and Sinninghe Damsté, J.
632 S.: Disentangling the origins of branched tetraether lipids and crenarchaeol in the lower Amazon river: Implications for
633 GDGT-based proxies, Limnol. Ocean., 58(1), 343–353, doi:10.4319/lo.2013.58.1.0343, 2013.
634 Zell, C., Kim, J. H., Balsinha, M., Dorhout, D., Fernandes, C., Baas, M. and Sinninghe Damsté, J. S.: Transport of branched
635 tetraether lipids from the Tagus River basin to the coastal ocean of the Portuguese margin: Consequences for the
636 interpretation of the MBT'/CBT paleothermometer, Biogeosciences, 11(19), 5637–5655, doi:10.5194/bg-11-5637-2014,
637 2014.
638 Zheng, Y., Pancost, R. D., Liu, X., Wang, Z., Naafs, B. D. A., Xie, X., Liu, Z., Yu, X. and Yang, H.: Atmospheric
639 connections with the North Atlantic enhanced the deglacial warming in northeast China, Geology, 45(11), 1031–1034,
640 doi:10.1130/G39401.1, 2017.
641

https://doi.org/10.5194/bg-2019-500
Preprint. Discussion started: 11 March 2020

642

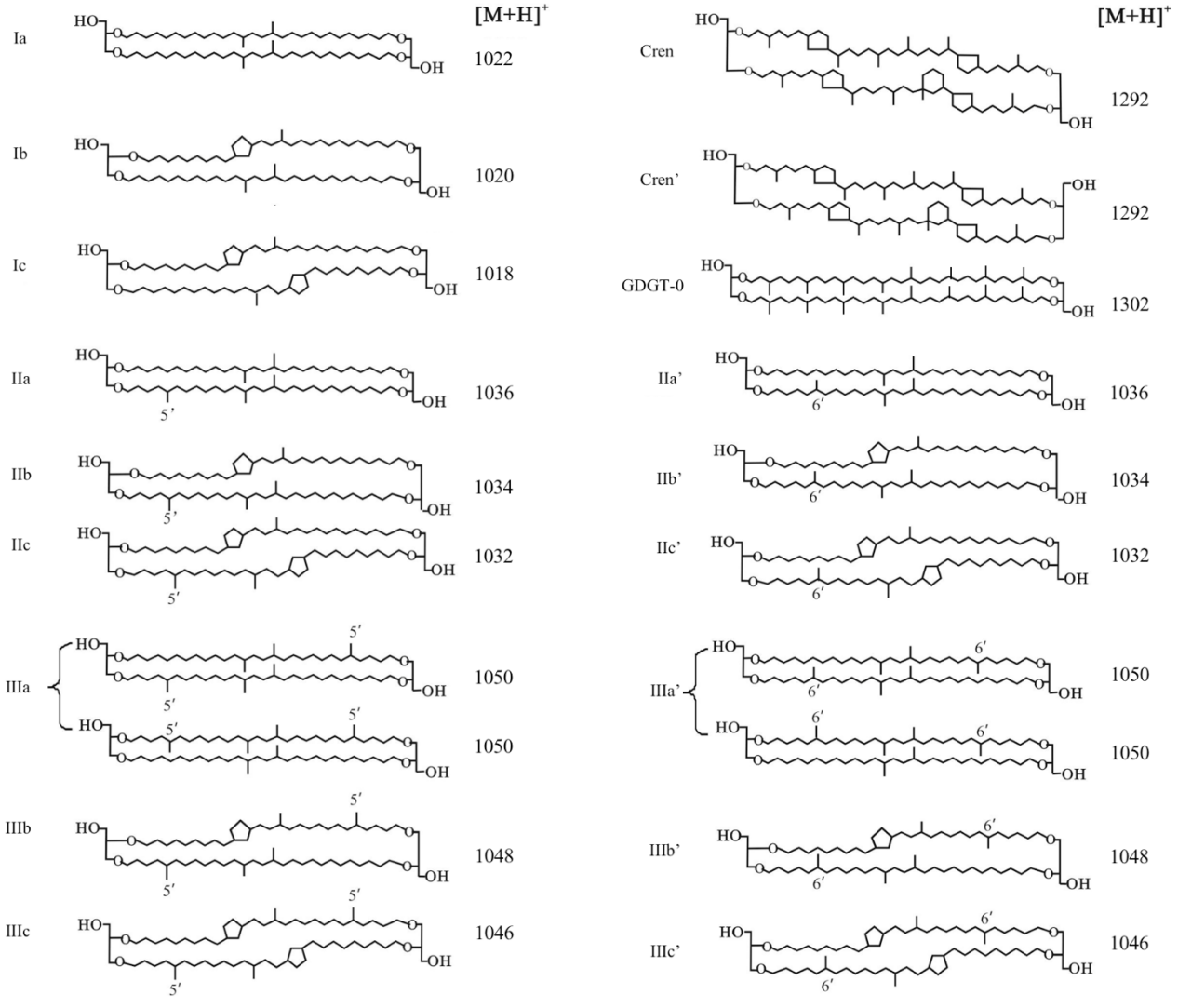

643

644 **Figure 1: Molecular structures of 5-methyl and 6-methyl branched GDGTs, GDGT-0 and crenarchaeol. The 6-methyl brGDGTs**
645 **are represented by apostrophe. The structures of penta- and hexamethylated brGDGTs with cyclopentane moiety(ies) IIb', IIc',**
646 **IIIb', IIIc' are tentative.**

https://doi.org/10.5194/bg-2019-500
Preprint. Discussion started: 11 March 2020

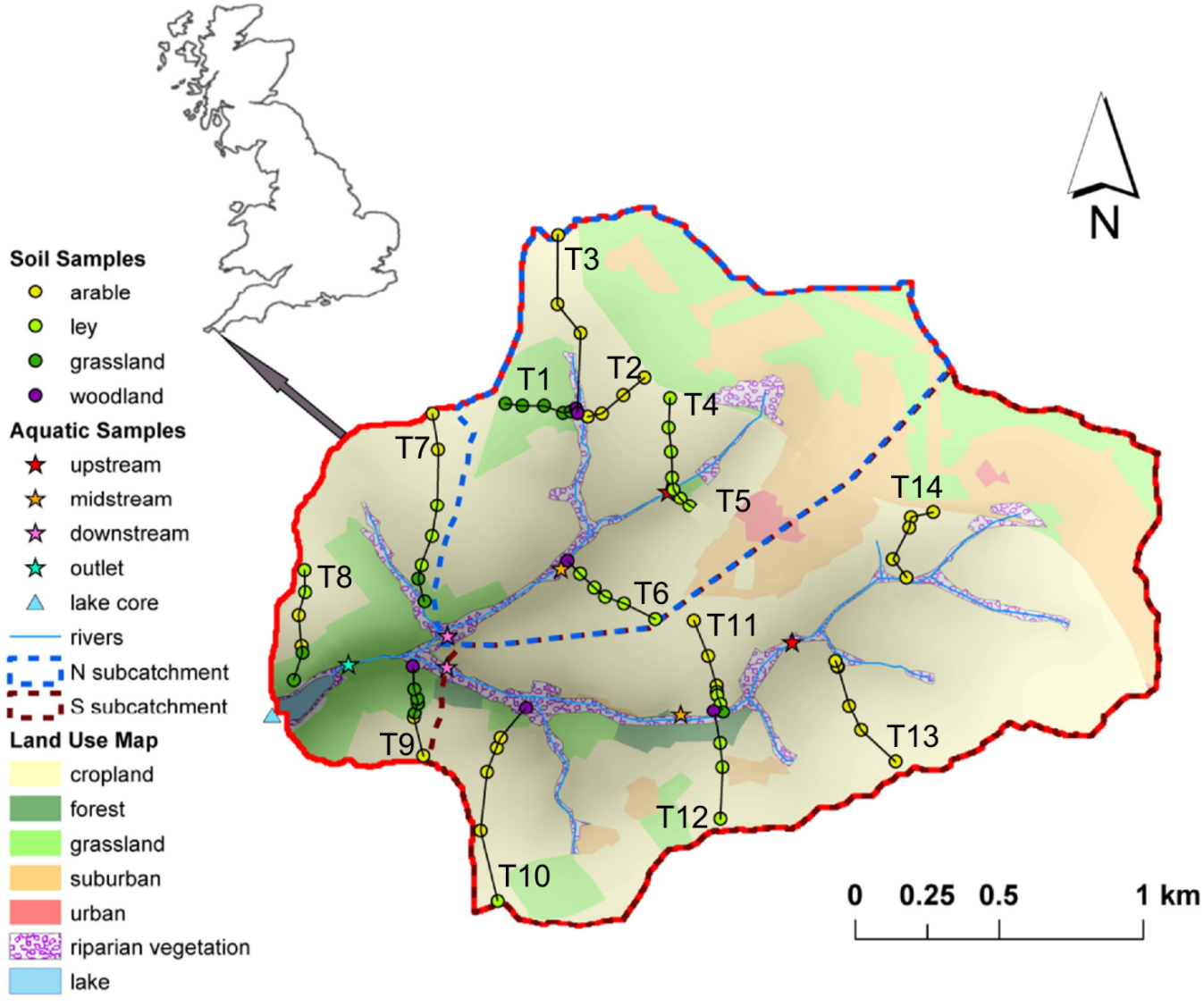

Figure 2: Map of the Carminowe Creek catchment in southwest England showing land use types, 14 soil transects (labelled T1-14), creek bed and lake core sediment sampling locations. The coloured circles and stars indicate soil samples under different land use types and creek bed sediments along the streams, respectively. Adjusted from Glendell et al. (2018).

https://doi.org/10.5194/bg-2019-500
Preprint. Discussion started: 11 March 2020

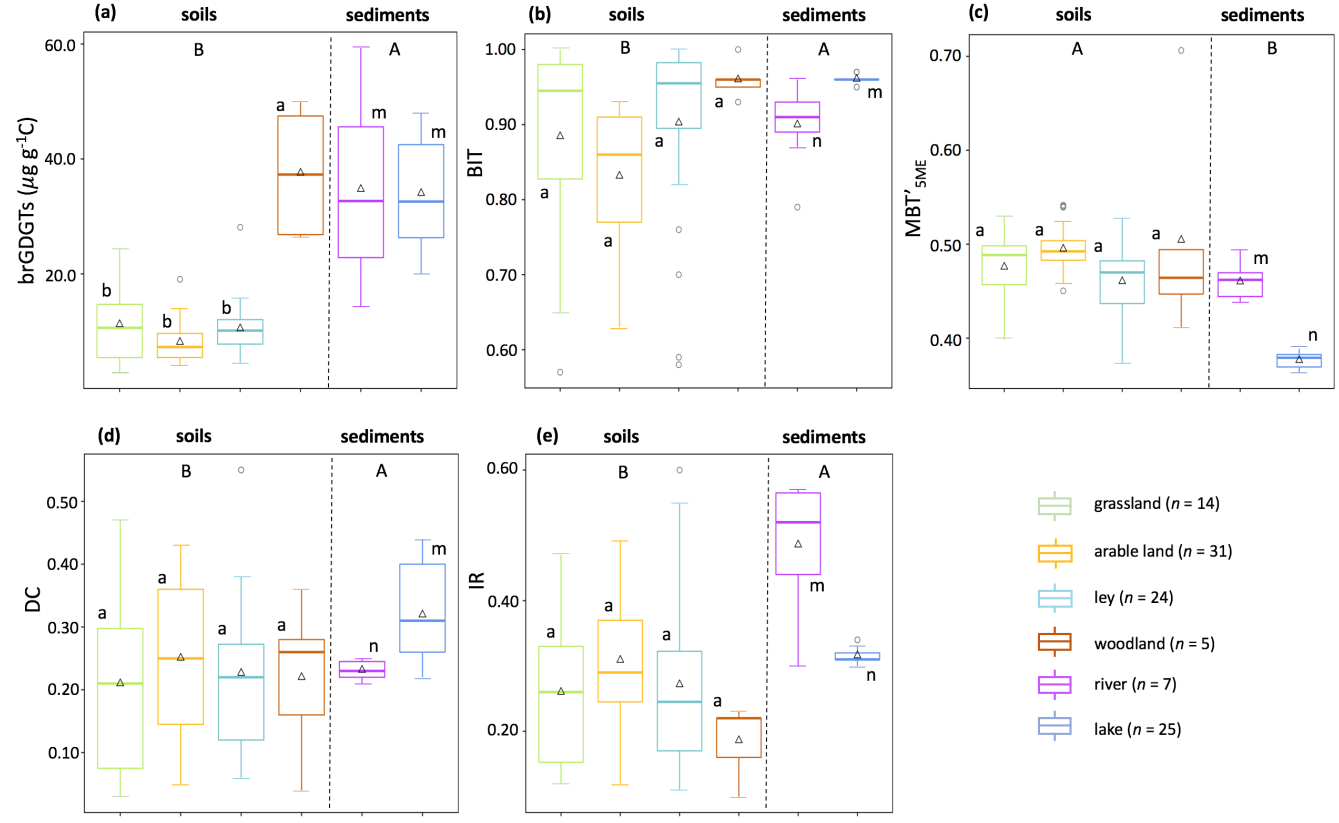

Figure 3: Box plots displaying (a) the C-normalized concentration of brGDGTs, and brGDGT-based indices: (b) BIT index (branched and isoprenoid tetraether ratio), (c) MBT'$_{5ME}$ (methylation of 5-methyl branched tetraethers), (d) DC (degree of cyclization) and (e) IR (isomerization ratio). The triangles represent the average values, the bold line indicates the median (50th percentile), bottom and top of the box indicate first quartile (25th percentile) and third quartile (75th percentile) respectively, whiskers cover the smallest and largest value within 1.5 times of the interquartile range (i.e. the distance between the top and bottom of the box). Any data points outside the whiskers are considered as outliers. Different letters indicate differences between samples: A and B for differences between catchment soils and aquatic sediments, a and b for soils under different vegetation types, and m and n for creek bed and lake core sediments ($p < 0.05$).

https://doi.org/10.5194/bg-2019-500
Preprint. Discussion started: 11 March 2020

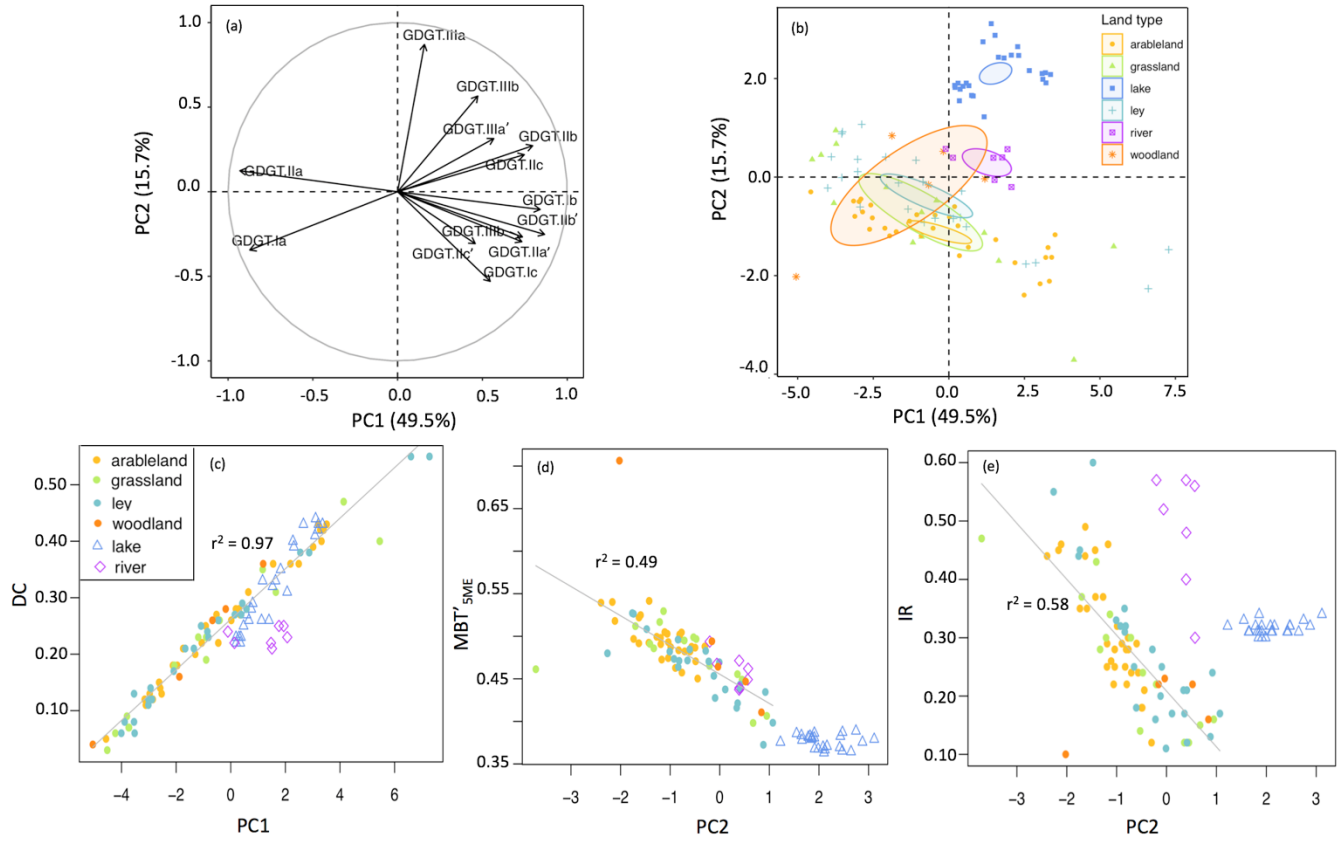

Figure 4: PCA based on the relative abundances of 13 major brGDGTs. Figure (a) shows the distribution of 13 brGDGTs (brGDGT-IIIc and brGDGT-IIIc' are excluded as they are below the detection limit) along the first two PCs, roman numerals and English alphabet represent the compounds shown in the Fig. 2. Figure (b) shows sampling sites loading scores on the first two PCs and 95% confidence ellipses around the categories of land use: arable land (*n* = 31), grassland (*n* = 14), ley (*n* = 24) and woodland (*n* = 5), and creek (*n* = 7) and lake (*n* = 25). Figure (c) shows cross plots between PC1 and DC (degree of cyclization). Figure (d) and (e) show cross plots of PC2 with MBT'_{5ME} (methylation of 5-methyl branched tetraethers) and IR (isomerization ratio) respectively. The linear correlation was calculated excluding creek and lake sediment.

https://doi.org/10.5194/bg-2019-500
Preprint. Discussion started: 11 March 2020

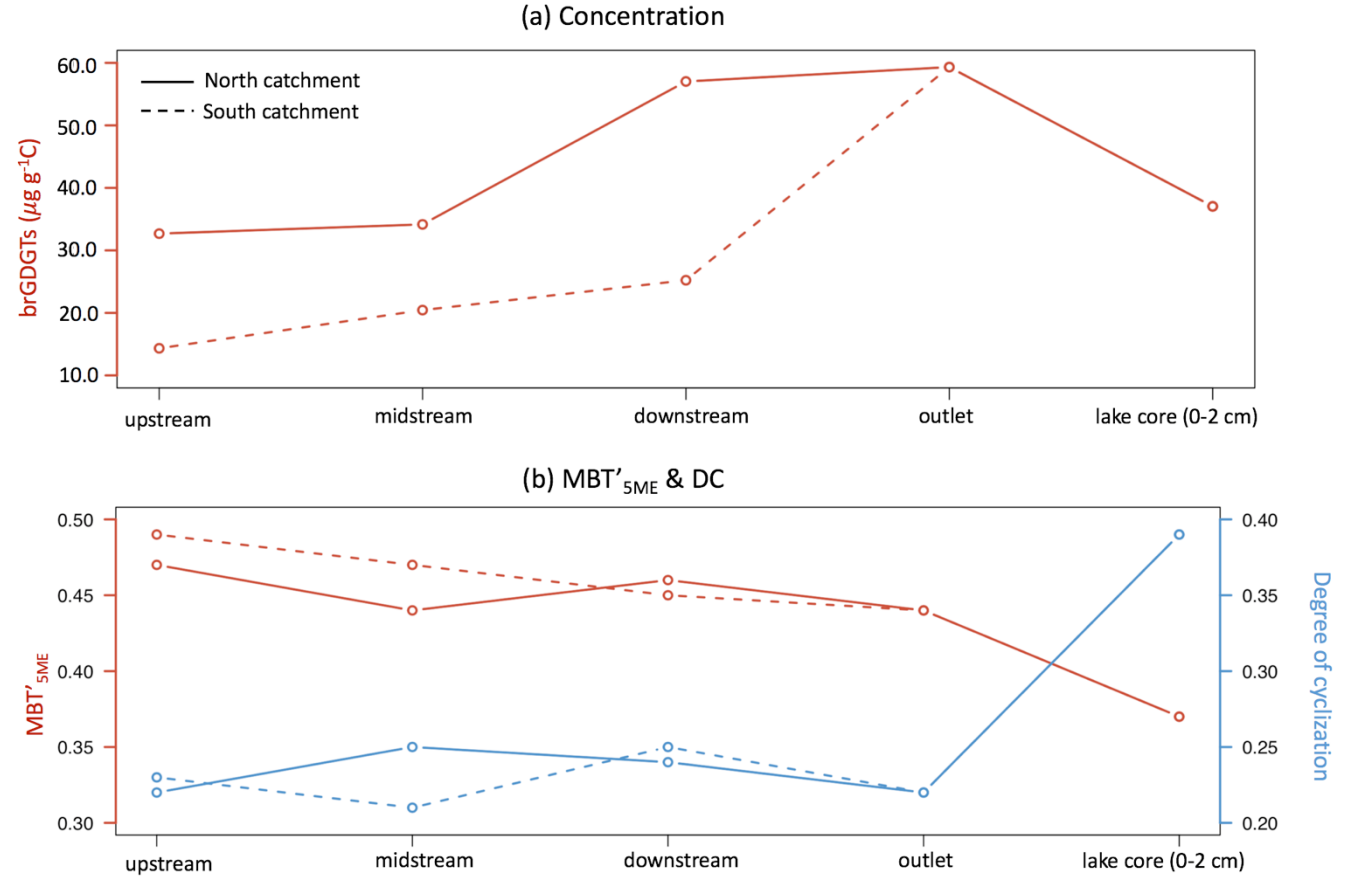

Figure 5: Spatial variability of (a) C-normalized concentration of brGDGTs and (b) MBT'$_{5ME}$ (methylation of 5-methyl branched tetraethers) and DC (degree of cyclization) in downstream direction of both substreams in the Carminowe Creek catchment.

https://doi.org/10.5194/bg-2019-500
Preprint. Discussion started: 11 March 2020

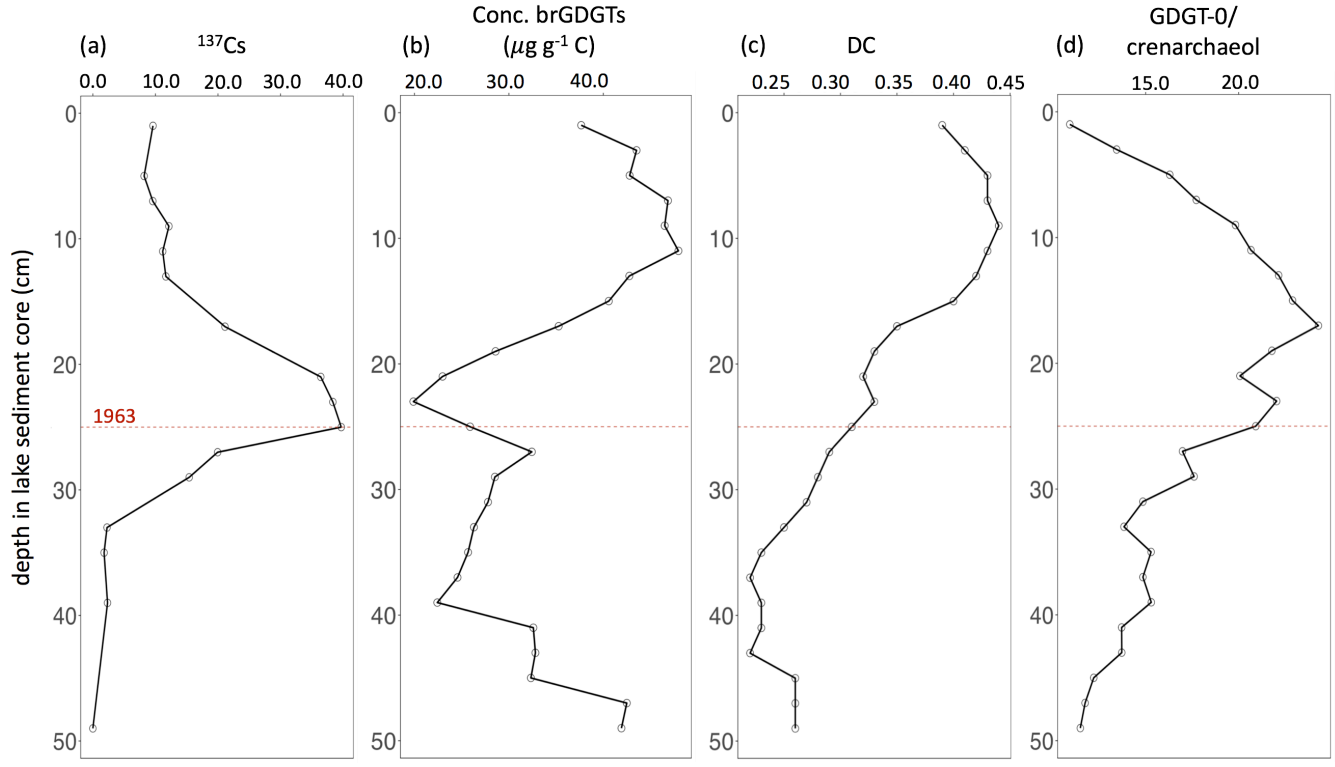

671

672 **Figure 6: Lake sediment core profiles of (a) ^{137}Cs to date, (b) C-normalized concentration of brGDGTs, (c) DC (degree of**
673 **cyclization) and (d) ratio between GDGT-0 and crenarchaeol. The red dashed line indicates the year of 1963.**

https://doi.org/10.5194/bg-2019-500
Preprint. Discussion started: 11 March 2020

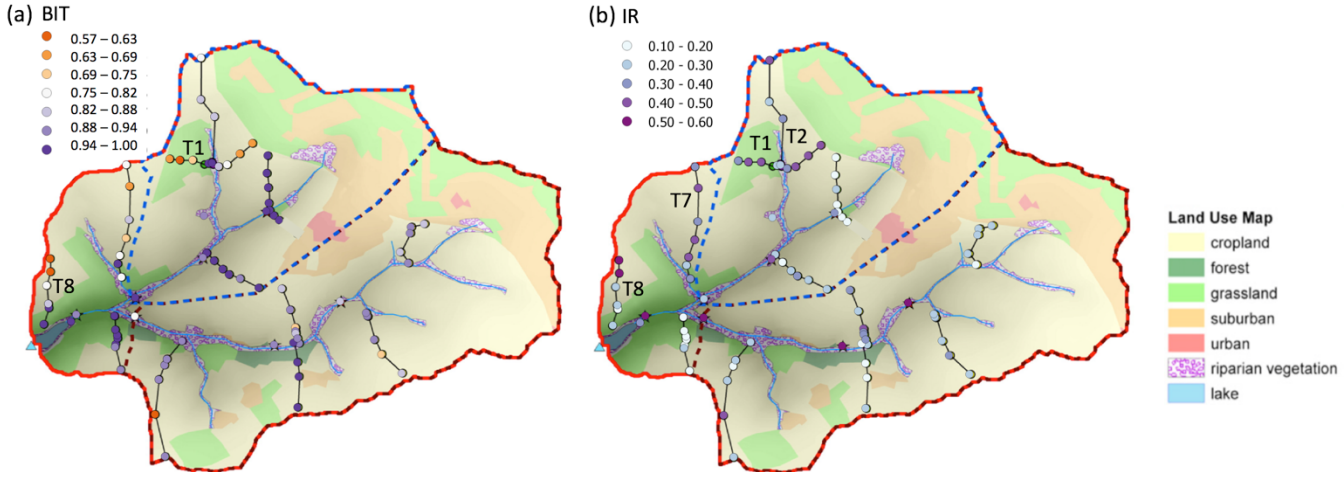

Appendix: Spatial variability of the (a) BIT (branched and isoprenoid tetraether ratio) and (b) IR (isomerization ratio) along 14 soil transects in the Carminowe Creek catchment. The coloured circles show the concentrations and proxy values. Tx indicates soil transects discussed in the text. The background colours indicate different land use types. Adjusted from Glendell et al. (2018).

https://doi.org/10.5194/bg-2019-500
Preprint. Discussion started: 11 March 2020

Biogeosciences Discussions Open Access EGU

Table 1. **C% (carbon content), pH values, average concentrations of brGDGTs and brGDGT-based indices under different land use types. BIT (branched and isoprenoid tetraether ratio), MBT'$_{5ME}$ (methylation of 5-methyl branched tetraethers), %tetra (percentage of tetramethylated brGDGTs), %penta (percentage of pentamethylated brGDGTs), %hexa (percentage of hexamethylated brGDGTs), DC (degree of cyclization), IR (isomerization ratio) (mean ± standard deviation, s.d.).**

Land use (n)	C% *	pH	Conc. (μg g^{-1} soil)	Conc. (μg g^{-1} C)	BIT	MBT'$_{5ME}$	%tetra	%penta	%hexa	DC	IR
arable (31)	2.9 ± 0.5	6.6 ± 0.4	0.2 ± 0.1	8.1 ± 3.6	0.83 ± 0.09	0.50 ± 0.02	40.1 ± 3.1	49.7 ± 1.5	10.2 ± 1.8	0.25 ± 0.11	0.31 ± 0.10
grass (14)	5.6 ± 1.2	6.0 ± 0.5	0.6 ± 0.4	11.2 ± 6.7	0.88 ± 0.14	0.48 ± 0.04	39.8 ± 4.0	49.4 ± 2.3	10.8 ± 2.1	0.21 ± 0.14	0.26 ± 0.12
ley (24)	3.6 ± 0.9	6.0 ± 0.3	0.4 ± 0.3	10.5 ± 4.8	0.90 ± 0.12	0.46 ± 0.04	37.8 ± 3.7	50.2 ± 2.0	12.0 ± 2.9	0.23 ± 0.14	0.27 ± 0.13
woodland (5)	8.2 ± 2.1	5.4 ± 0.7	3.0 ± 1.0	37.6 ± 11.0	0.96 ± 0.03	0.50 ± 0.12	45.4 ± 13.0	44.4 ± 8.3	10.3 ± 4.8	0.22 ± 0.12	0.19 ± 0.05
all soils (74)	4.0 ± 1.8	6.2 ± 0.5	0.6 ± 0.8	11.5 ± 8.9	0.87 ± 0.12	0.48 ± 0.04	39.7 ± 4.9	49.4 ± 3.0	10.9 ± 2.6	0.23 ± 0.13	0.28 ± 0.11
creek (7)	2.3 ± 0.8	7.1 ± 0.2	0.8 ± 0.4	34.7 ± 17.4	0.90 ± 0.06	0.46 ± 0.02	30.1 ± 4.5	45.0 ± 0.7	24.9 ± 4.7	0.23 ± 0.02	0.48 ± 0.10
Lake (25)	7.5 ± 1.0	5.7 ± 0.2	2.6 ± 0.7	34.0 ± 8.7	0.96 ± 0.01	0.38 ± 0.01	28.9 ± 0.7	50.2 ± 1.8	21.0 ± 1.4	0.32 ± 0.08	0.32 ± 0.01

678 *From Glendell et al. (2018)